Design, Synthesis, and Pharmacological Evaluation of Conformationally Constrained Analogues of *N*,*N*′-Diaryl- and *N*-Aryl-*N*-aralkylguanidines as Potent Inhibitors of Neuronal Na^+ Channels

Michel C. Maillard,*,§ Michael E. Perlman,§ Oved Amitay,‡ Deborah Baxter,‡ David Berlove,‡ Sonia Connaughton,‡ James B. Fischer,‡ Jun Qing Guo,§ Lain-Yen Hu,§ Robert N. McBurney, Peter I. Nagy,† Katragadda Subbarao,‡ Elizabeth A. Yost,§ Lu Zhang,§ and Graham J. Durant§

Cambridge NeuroScience Inc., One Kendall Square, Cambridge, Massachusetts 02139

Received February 24, 1998

In the present investigation, the rationale for the design, synthesis, and biological evaluation of potent inhibitors of neuronal Na^+ channels is described. *N*,*N*′-Diaryl- and *N*-aryl-*N*-aralkylguanidine templates were locked in conformations mimicking the permissible conformations of the flexible diarylguanidinium ion (AS^+, AA^+, SS^+). The resulting set of constrained guanidines termed "lockamers" (cyclophane, quinazoline, aminopyrimidazolines, aminoimidazolines, azocino- and tetrahydroquinolinocarboximidamides) was examined for neuronal Na^+ channel blockade properties. Inhibition of [^{14}C]guanidinium ion influx in CHO cells expressing type IIA Na^+ channels showed that the aminopyrimidazoline **9b** and aminoimidazoline **9d**, compounds proposed to lock the *N*,*N*′-diarylguanidinium in an SS^+ conformation, were the most potent Na^+ channel blockers with IC_{50}'s of 0.06 μM, a value 17 times lower than that of the parent flexible compound **18d**. The rest of the restricted analogues with 4-*p*-alkyl substituents retained potency with IC_{50} values ranging between 0.46 and 2.9 μM. Evaluation in a synaptosomal $^{45}Ca^{2+}$ influx assay showed that **9b** did not exhibit high selectivity for neuronal Na^+ vs Ca^{2+} channels. The retention of significant neuronal Na^+ blockade in all types of semirigid conformers gives evidence for a multiple mode of binding in this class of compounds and can possibly be attributed to a poor structural specificity of the site(s) of action. Compound **9b** was also found to be the most active compound in vivo based on the high level of inhibition of seizures exhibited in the DBA/2 mouse model. The pK_a value of **9b** indicates that **9b** binds to the channel in its protonated form, and log *D* vs pH measurements suggest that ion-pair partitioning contributes to membrane transport. This compound stands out as an interesting lead for further development of neurotherapeutic agents.

Introduction

Voltage-dependent Na^+ channel blockers are widely used as local anesthetics, antiarrhythmics, and anticonvulsant agents.[1,2] In the past few years, the potential role of this pharmacological class of agents has been extensively investigated in various disorders of the central and peripheral nervous systems such as stroke, head trauma, spinal cord injury, neuropathic pain, and amyotrophic lateral sclerosis (ALS).[2−5]

It has been proposed that, in ischemic situations such as stroke or head trauma, the development of Na^+ channel hyperactivity is implicated in the cascade of biochemical events that ultimately lead to neuronal cell death.[2,3,6] This hypothetical mechanism has provided a basis for the evaluation of Na^+ channel blockers in experimental models of ischemic stroke. Tetrodotoxin, a marine toxin that selectively blocks voltage-dependent Na^+ channels, was found to be neuroprotective in a model of global brain ischemia,[7] substantiating the pathophysiological role of voltage-dependent Na^+ channels under ischemic conditions. In addition, Na^+ channel blockers, which have shown to prevent hypoxic damage to mammalian white matter in isolated optic nerve, offer advantages over other neuroprotective agents active only in gray matter.[6b,c] Thus, considerable effort has been devoted to identifying novel selective voltage-dependent Na^+ channel antagonists with acceptable brain permeability. These investigations have led to the study of a number of these derivatives (Chart 1) in clinical trials for acute treatment of cerebral ischemia.[8] More recently, we reported[9] the in vivo efficacy of the *N*,*N*′-diarylguanidine Na^+ channel blocker CNS 1237 (Chart 1) in a model of focal cerebral ischemia, and the anticonvulsant agent carbamazepine (Chart 1) has also proven to be beneficial in experimental models of cerebral ischemia.[10]

However, a number of these derivatives such as CNS 1237, lifarizine, and lubeluzole also interact strongly with voltage-dependent Ca^{2+} channels, which may be linked in part to their anti-ischemic properties.[11] Other findings suggest, however, that the relevance of voltage-activated Ca^{2+} channel blockade to the neuroprotective action of these agents is uncertain.[12] Moreover, L-type and N-type[13] Ca^{2+} channel blockers are known to have profound hypotensive effects, and neuronal voltage-dependent P-type Ca^{2+} channel antagonists have been

* To whom correspondence should be addressed. Current address: Athena Neurosciences, Inc., 800 Gateway Blvd, South San Francisco, CA 94080.
§ Department of Chemistry.
‡ Department of Pharmacology.
† Center for Drug Design and Development, Department of Medicinal and Biological Chemistry, University of Toledo, Toledo, OH.

S0022-2623(98)00124-1 CCC: $15.00
Published on Web 07/03/1998

Chart 1. Structure of Several Neuronal Na^+ Channel Blockers and Mixed Na^+ and Ca^{2+} Channel Blockers

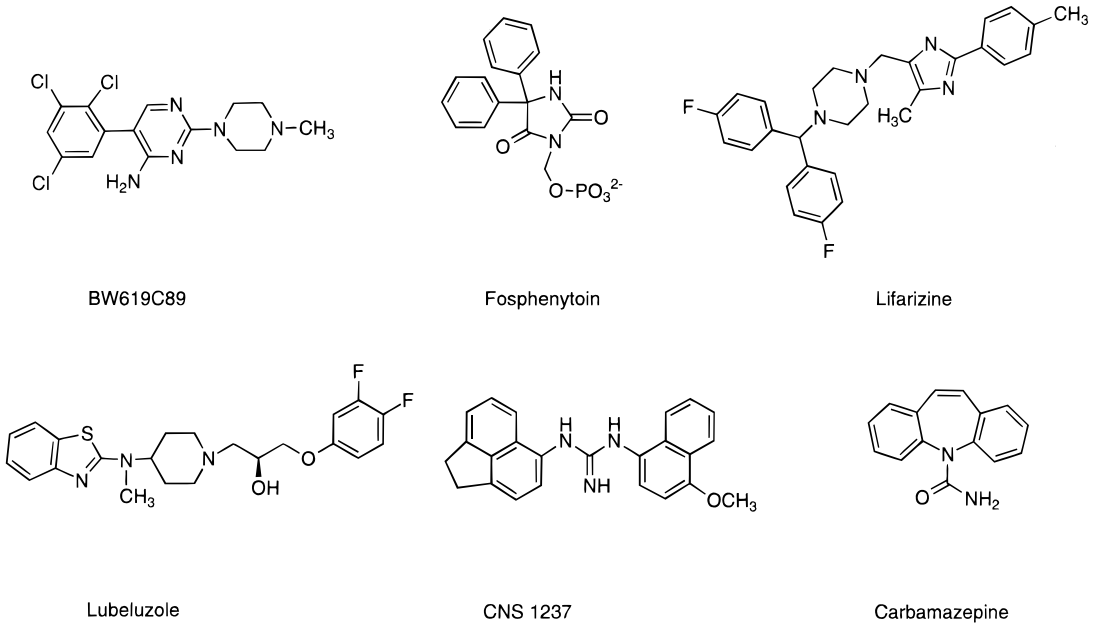

shown to prevent transmitter release at the mammalian neuromuscular junction, which can potentially cause muscle paralysis.[14] We therefore attempted to develop potent and selective neuronal Na^+ channel blockers from our series of *N*,*N*′-diarylguanidines.

The dual action on both Na^+ and Ca^{2+} channels of *N*,*N*′-diarylguanidines related to CNS 1237 is not surprising since these compounds are conformationally flexible and can potentially interact with multiple ion-channel types and subtypes with different topologies. Thus, an approach based on conformationally restricted analogues could be valuable for identifying selective agents more potent than flexible compounds. Additionally, such restricted analogues should serve as molecular tools, providing geometrical information on the pharmacophoric elements of the channel-bound conformation of *N*,*N*′-diarylguanidines.

In this paper, we report the design, synthesis, and in vitro evaluation of conformationally restricted analogues of *N*,*N*′-diphenyl- and *N*-phenyl-*N*-benzylguanidines. We discuss relationships of conformation to activity and structure−activity relationships that govern their Na^+ channel blockade properties. For the most potent analogues, in vivo activities and physicochemical data that pertain to central activity are also reported.

Design Rationale

Conformational analysis of the protonated form of *N*,*N*′-diarylguanidines, which is believed to be the active species of the compounds under physiological conditions, has been the subject of previous investigations.[15,16] In Figure 1 are two-dimensional representations of the three possible conformational classes of the *N*,*N*′-diphenylguanidinium ion: (i) anti−anti$^+$ (AA^+), (ii) anti−

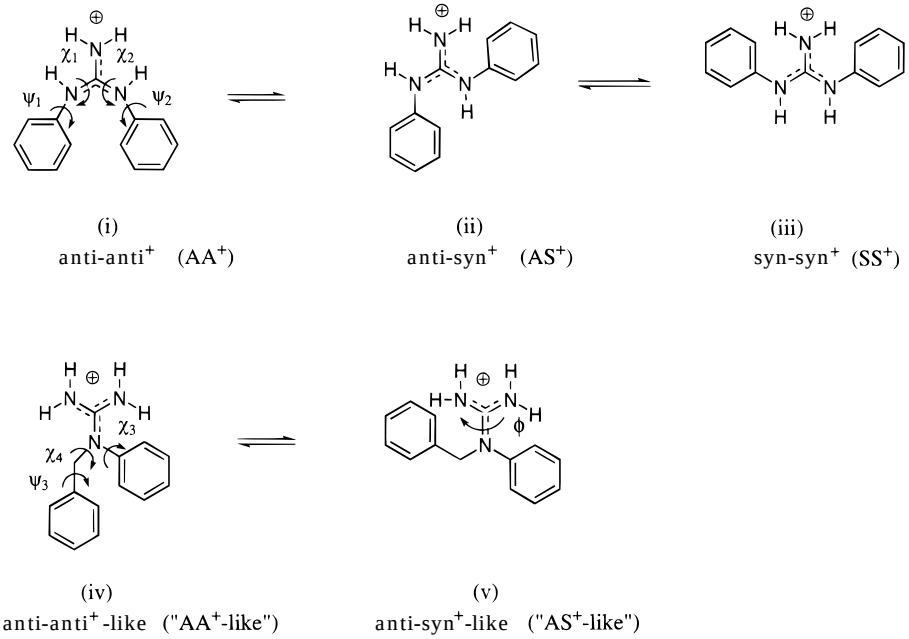

Figure 1. Three possible conformational classes of symmetrical *N*,*N*′-diarylguanidinium ion (i, ii, iii) and two possible conformational classes of *N*-aryl-*N*-aralkylguanidinium ion (iv, v).

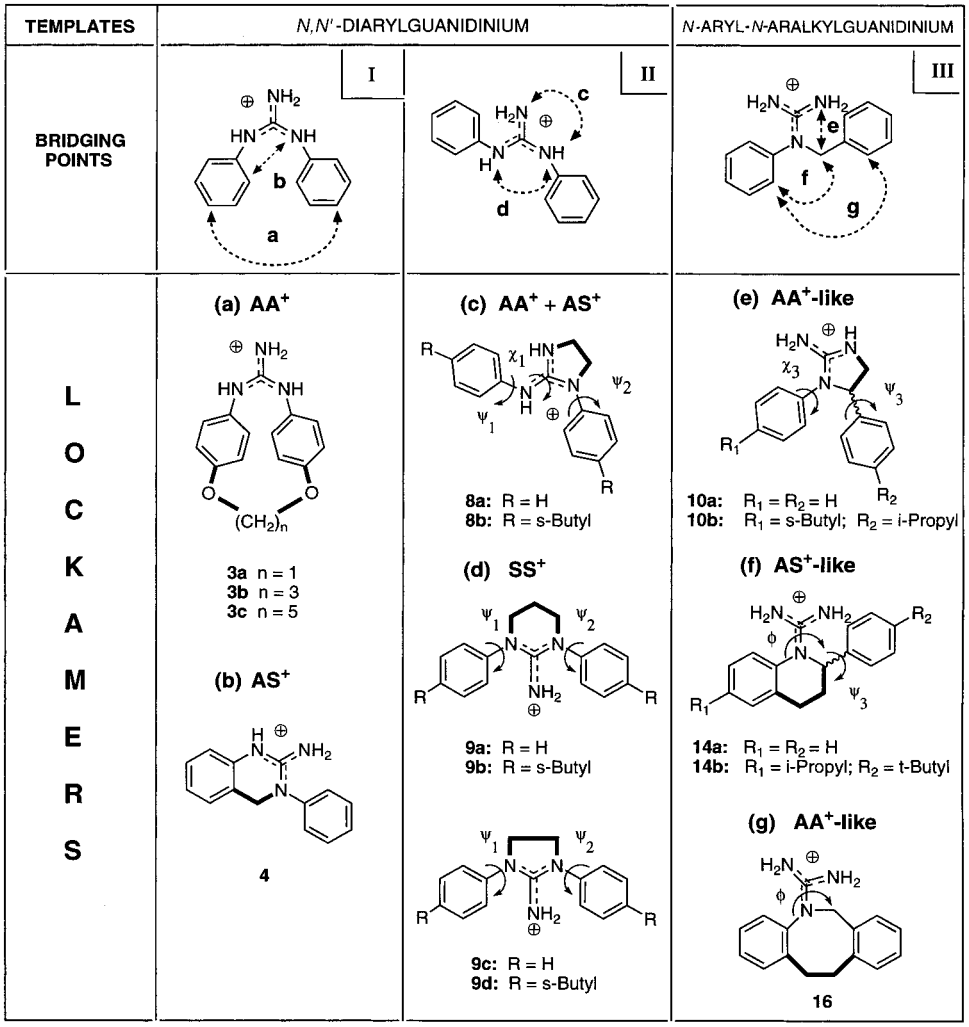

Figure 2. Structures of templates and "lockamers" including cyclization strategies **a**−**g**. Tether bonds are shown in bold, and unrestrained torsional angles ψ_{1-3}, χ_{1-3}, and ϕ are delineated with curved arrows.

syn$^+$ (AS$^+$), and (iii) syn−syn$^+$ (SS$^+$). Torsion angles χ_1 and χ_2 govern the syn−anti isomerism while ψ_1 and ψ_2 define the position of each phenyl ring relative to the plane of the guanidinium function. In its bioactive form the *N*,*N*′-diphenylguanidinium cation is expected to be bound via an electrostatic interaction to a carboxylate residue of the ion channel. For modeling this situation, Monte Carlo simulation of the counterion effect on the conformational equilibrium of the *N*,*N*′-diphenylguanidinium ion was carried out with an acetate counterion as a possible mimic for the carboxylate group.[16] This study revealed an apparent energetic accessibility of the three conformers, which should result in significant populations under physiological conditions. These results encouraged us to investigate the well-established principle of conformational restraint as an approach to optimizing Na^+ channel blockade properties. This approach targeted, separately or in combination, the AS$^+$, SS$^+$, and AA$^+$ forms as hypothetical bioactive conformations of these neuronal Na^+ channel blockers.

Seven cyclization strategies were considered for locking the conformation of *N*,*N*′-diaryl- and *N*-aryl-*N*-aralkylguanidines into the targeted conformationally restricted analogues ("lockamers").[17] These seven cyclization strategies are depicted in Figure 2 as paths a−g and are presented in three groups (I−III) depending on the nature of the structural base and the location of the bridging points of the tether. The first two groups (I, II) utilize the *N*,*N*′-diarylguanidine template and include four cyclization strategies (a−d); these strategies enabled us to access "lockamers" representing one or two of the conformers (i−iii) described in Figure 1. The third group (III) involves an *N*-aryl-*N*-aralkylguanidine template and includes three cyclization strategies (e−g). We chose this second template because it allows access to restricted analogues based on the rotamers (iv and v) (Figure 1) which mimic respectively the AA$^+$ and AS$^+$ conformations of the *N*,*N*′-diarylguanidinium. In the first group (I), rigidification was achieved by either bridging the two para positions (path a) or linking an ortho position with a nitrogen atom (path b), whereas only nitrogen atoms were used as anchor points for the tether (paths c, d) in the second group (II). Finally, in the third group (III), the following positions were utilized as anchor points: (e) a nitrogen atom and the benzylic carbon, (f) an ortho aromatic carbon and the benzylic carbon, (g) ortho carbons of both aromatic rings. Arrows accompanying the templates I−III in Figure 2 delineate the bridging points, and tether bonds are shown in bold in compounds **3a**−**c**, **4**, **8a**,**b**, **9a**−**d**, **10a**,**b**, **14a**,**b**, and **16**.

Analogues **3a**−**c** are locked in a geometric arrangement in which the two phenyl rings are restricted in

Scheme 1[a]

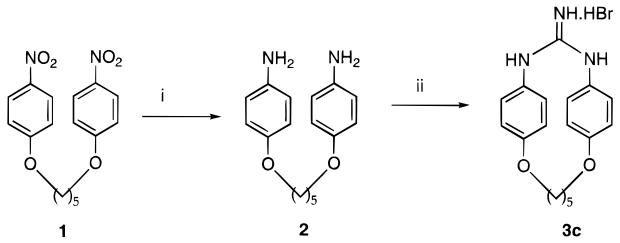

[a] (i) H_2, Pd/C (10%), EtOH; (ii) BrCN, EtOH.

an AA^+ conformation. The choice of the tether's length was supported by molecular mechanics calculations for the protonated cations **3a**−**c** using the AMBER*/Macromodel 6.0 force field.[19] These calculations indicated that the seven-atom tether of compound **3c** was the minimum tether length at which no distortions of the overall geometry were observed compared to that for the flexible analogue **18c** in the AA^+ conformation (see the Experimental Section for details). Restriction of the *N*,*N*′-diarylguanidine template with a methylene tether according to path b affords the 2-amino-3-*N*-phenylquinazoline "lockamer" **4** which approximates an AS^+ conformation. A two-carbon-atom tether between an aryl-substituted nitrogen and a nonsubstituted nitrogen gives **8a**,**b** (path c). This type of "lockamer" is more flexible than **3c** and **4**, having access to both AA^+ and AS^+ conformational domains without conformational restriction on the aromatic rings. Similarly, a two- or three-carbon-atom tether between the two aryl-substituted nitrogen atoms yields **9a**−**d**, which are locked in SS^+ conformations (path d).

The *N*-aryl-*N*-aralkylguanidine template was rigidified by linking a nonsubstituted nitrogen to the benzylic carbon with a methylene bridge (path e), creating an imidazoline scaffold **10a**,**b** that mimics AA^+ conformations of *N*,*N*′-diarylguanidines ("AA^+-like"). The possible conformations of compounds **10a**,**b** resemble AA^+ conformations i (Figure 1) since the two aromatic rings point away from the same side of the guanidine moiety. However, in this variant, torsion angles ψ_3 and χ_3 are unrestrained, allowing rotation of both aromatic rings. At this point, it is important to note that in these four imidazoline- and pyrimidazoline-based scaffolds (**8a**,**b**, **9a**,**b**, **9c**,**d**, **10a**,**b**), the torsion angles ψ_1, ψ_2, ψ_3, and χ_3, which define the orientation of the two aromatic groups relative to the plane of the guanidinium moiety, remain unrestrained but the guanidine moiety is embedded in the scaffold.

The design considerations for the next stage were then twofold. First, we wanted to liberate the guanidino function from being embedded in the scaffold. Its cyclic nature could dramatically change physicochemical properties such as the pK_a, log *D*, and hydrogen-bonding properties which could have some major implications on the ability of the rigid variant to become protonated at physiological pH or to cross the blood−brain barrier (BBB). Second, we wanted to impose, separately, a different degree of constraint on each aromatic group. With these considerations in mind, the *N*-aryl-*N*-aralkylguanidine template (III) was utilized to design the novel guanidine variants **14a**,**b** and **16** by varying the ethylene tether's points of substitution (paths f, g). These two compounds would mimic, respectively, AS^+ and AA^+ conformations of the *N*,*N*′-diarylguanidinium ion and satisfy both design criteria. For compounds **14a**,**b** ("AS^+-like"), ϕ and ψ_3 torsion angles are conformationally unrestrained, allowing torsional motion of the *N*-carboximidamide and of an aromatic ring, respectively. In the case of compound **16** ("AA^+-like"), conformational variability resides in rotation of the *N*-carboximidamide (ϕ) and flexing of the tricyclic ring.

Previous structure−activity relationship (SAR) studies of *N*,*N*′-diarylguanidines[20] and *N*-aryl-*N*-aralkylguanidines[21] revealed that large alkyl and alkoxy groups (isobutyl, isopropyl, *n*-butoxy) were preferred on the phenyl rings for Na^+ channel blockade, with the para substitution being especially advantageous. Nonsubstituted derivatives were devoid of activity. In this work, we set out to prepare both nonsubstituted and

Scheme 2[a]

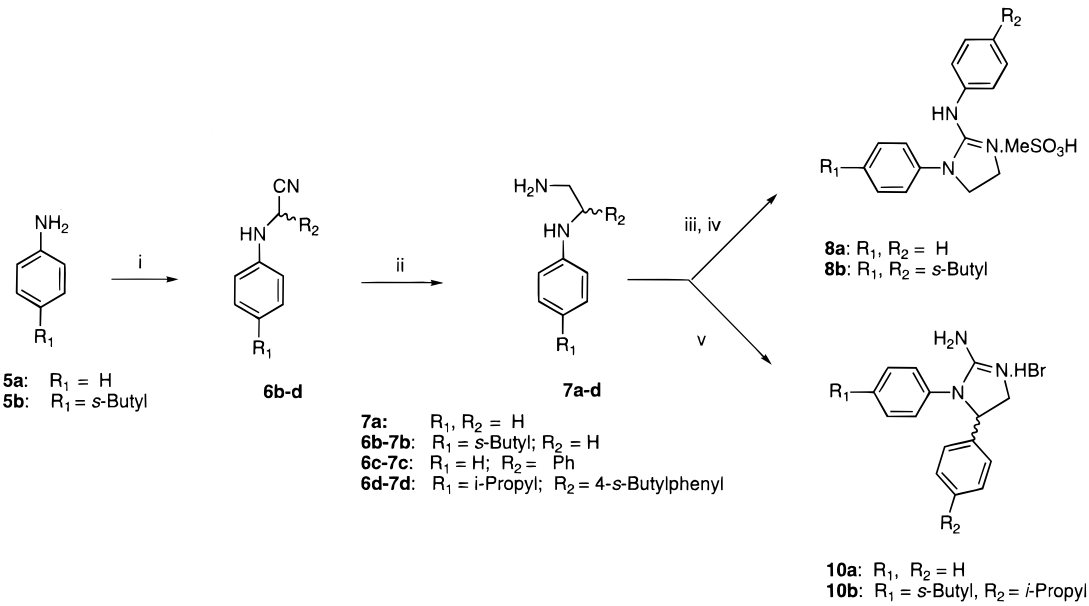

[a] (i) $NaHSO_3/R_2CHO$, KCN, $AcOH/H_2O$; (ii) H_2, 50 psi, Raney Ni, NH_3/EtOH; (iii) (for **7a**,**b**) CS_2, EtOH then MeI; (iv) **5a** or **5b**, neat, Δ; (v) (for **7c**,**d**) BrCN, EtOH, Δ.

Scheme 3[a]

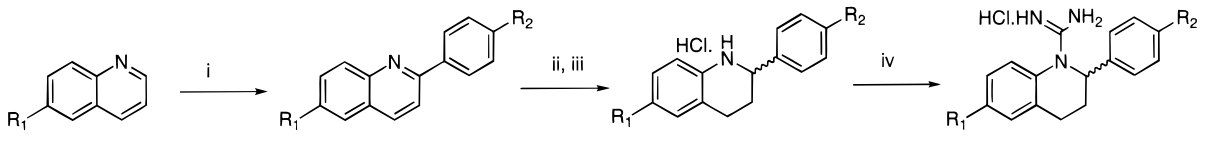

11b: R_1 = i-Propyl

12a: R_1, R_2 = H
12b: R_1 = i-Propyl; R_2 = t-Butyl

13a: R_1, R_2 = H
13b: R_1 = i-Propyl ; R_2 = t-Butyl

14a: R_1, R_2 = H
14b: R_1 = i-Propyl; R_2 = t-Butyl

[a] (i) Aryllithium, THF; (ii) H_2, 50 psi, PtO_2, EtOH; (iii) 1 N HCl, Et_2O; (iv) NH_2CN, EtOH.

Scheme 4[a]

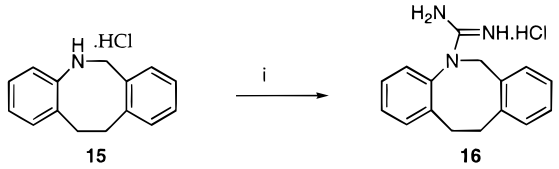

15 **16**

[a] (i) NH_2CN, EtOH.

p-alkyl- or *p*-alkoxy-substituted analogues of the "lockamers" previously defined. It was reasoned that a different SAR may apply in the semirigid series since correctly oriented nonsubstituted phenyls may significantly benefit activity by virtue of a more favorable entropy of binding. Substituted and nonsubstituted *N*,*N*′-diaryl- and *N*-aryl-*N*-aralkylguanidines **18a**−**d** and **20a**,**b** were also synthesized for establishing direct comparison with the rigid variants previously described.

Chemistry

The synthesis of several of the compounds in Figure 2 has been reported previously, including the aminoquinazoline **4**[22] and the aminopyrimidazolines and aminoimidazolines **9a**−**d**.[23] Guanidine **3c** was obtained in a two-step procedure described in Scheme 1. The dinitro derivative **1** was reduced by catalytic hydrogenation over Pd/C. The resulting diamine **2** was then treated with cyanogen bromide to generate a monocyanamide intermediate which was not isolated, and upon heating, this intermediate underwent intramolecular cyclization to form **3c**. Analogues **8a**,**b**[24] and **10a**,**b**[25] were prepared by minor variation of standard chemical routes illustrated in Scheme 2. The α-aminonitrile intermediates **6b**−**d** were obtained according to a modified Strecker reaction,[24,26] and hydrogenation to the diamines **7b**−**d** was carried out with Raney nickel in an ammonia-saturated ethanol solution.[27] The methylthiourea derivatives of **7a**,**b** were reacted respectively with **5a**,**b** in neat conditions to afford **8a**,**b**, whereas cyclization of **7c**,**d** by reaction with cyanogen bromide in ethanol provided **10a**,**b**.

The novel analogues **14a**,**b** were prepared from quinolines as outlined in Scheme 3. Reaction of quinoline **11b** with an aryllithium[28] yielded the 2-arylquinoline **12b** instead of the expected 2-aryl-1,2-dihydroquinoline. The quinolines **12a**,**b** were reduced by catalytic hydrogenation on platinum(IV) oxide[29] to afford the tetrahydroquinoline compounds **13a**,**b**. Compounds **13a**,**b** were then reacted with cyanamide to form the desired guanidines **14a**,**b**. Likewise, guanidine **16** was prepared from the commercially available azocine **15** (Scheme 4).

Symmetrical *N*,*N*′-diarylguanidines **18a**−**c** were readily obtained by directly reacting 2 equiv of the amines **17a**−**c** with 1 equiv of cyanogen bromide,

Scheme 5[a]

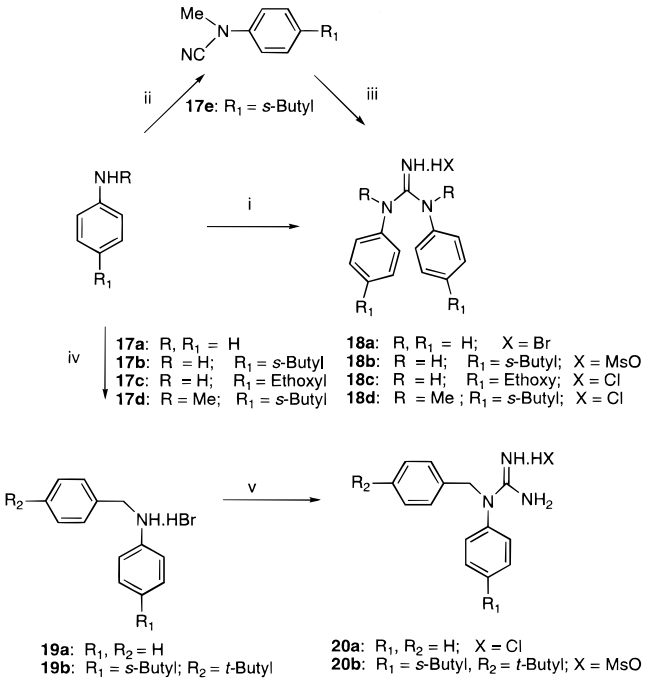

[a] (i) (For **17a**−**c**) 0.5 equiv of BrCN, EtOH; (ii) (for **17b**) BrCN, Et_2O then NaH, MeI, THF; (iii) $AlCl_3$, **17d**·HCl, toluene, Δ; (iv) (for **17a**,**b**) benzyl bromide, Et_3N, CH_2Cl_2; (v) NH_2CN, CH_2Cl_2 then NaOH and acid.

without isolating the intermediate cyanamide (Scheme 5).[30] Coupling of the amine hydrohalide salt of **17d**[31] with the arylalkylcyanamide **17e**, obtained from **17b** in two steps, furnished in the presence of $AlCl_3$[32] the symmetrical tetrasubstituted *N*,*N*′-diaryl-*N*,*N*′-dimethylguanidine **18d**. The *N*-aryl-*N*-aralkylguanidines **20a**,**b** were prepared by reacting the corresponding amines **19a**,**b** with cyanamide in chloroform. The amines **19a**,**b** were readily obtained by N-alkylation of the aniline derivatives **17a**,**b** with the appropriate benzyl bromide.

Biological Testing

The ability of our compounds to block voltage-activated neuronal Na^+ channels was determined in an in vitro functional assay employing a Chinese hamster ovary (CHO) cell line that stably expresses the cloned type IIA Na^+ channels derived from rat brain.[33] Type IIA Na^+ channels are the most abundant in rat brain[34] and are structurally and functionally related to human brain Na^+ channels.[35] The α-subunit, the principal component of the channel, behaves as a native Na^+ channel when expressed alone in CHO cells.[36] This evidence, supplemented by the finding that the guanidinium cation permeates through Na^+ channels which are opened by veratridine exposure,[37] strongly supports

Table 1. Summary of Results for [^{14}C]Guanidinium Flux Assay[a]

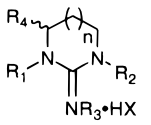

8a,b, 9a-d, 10a,b

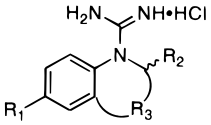

14a,b, 16

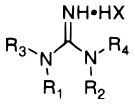

3c, 18a-d, 20a,b

compd	R_1	R_2	R_3	R_4	*n*	salt	Scheme	[^{14}C]guanidinium flux IC_{50}, μM ± SEM[b]
3c	−Ph(4)-O(CH_2)$_5$O-Ph(4)−		H	H		HBr	1	2.90 ± 0.67
4	(Figure 2)					HBr		9.95 ± 1.11
8a	Ph	H	Ph	H	0	$MeSO_3H$	2	>25
8b	Ph(4-*s*-Bu)	H	Ph(4-*s*-Bu)	H	0	$MeSO_3H$	2	0.78 ± 0.08
9a	Ph	Ph	H	H	1	HBr		>25
9b	Ph(4-*s*-Bu)	Ph(4-*s*-Bu)	H	H	1	HBr		0.06 ± 0.01
9c	Ph	Ph	H	H	0	HBr		14.68 ± 4.76
9d	Ph(4-*s*-Bu)	Ph(4-*s*-Bu)	H	H	0	HBr		0.06 ± 0.01
10a	Ph	H	H	Ph	0	HBr	2	>24
10b	Ph(4-*s*-Bu)	H	H	Ph(4-*i*-Pr)	0	HBr	2	1.80 ± 0.22
14a	H	Ph	−CH_2CH_2−			HCl	3	17.55 ± 1.34
14b	*i*-Pr	Ph(4-*t*-Bu)	−CH_2CH_2−			HCl	3	0.46 ± 0.07
16	H	H	−CH_2CH_2Ph(2)−			HCl	4	38.02 ± 5.21
18a	Ph	Ph	H	H		HBr	5	>14
18b	Ph(4-*s*-Bu)	Ph(4-*s*-Bu)	H	H		$MeSO_3H$	5	0.80 ± 0.08
18c	Ph(4-EtO)	Ph(4-EtO)	H	H		HCl	5	3.28 ± 0.31
18d	Ph(4-*s*-Bu)	Ph(4-*s*-Bu)	Me	Me		HCl	5	1.00 ± 0.16
20a	Ph	H	Bz	H		HCl	5	53.0 ± 6.0
20b	Ph(4-*s*-Bu)	H	Bz(4-*t*-Bu)	H		$MeSO_3H$	5	0.62 ± 0.11
CNS 1237	(Chart 1)					$MeSO_3H$		1.64 ± 3.85
lubeluzole	(Chart 1)					2HCl		0.26 ± 0.09
tetrodotoxin						2citrate		0.004 ± 0.001

[a] See the Experimental Section for details. [b] Values are means of at least three separate determinations ± SEM.

Table 2. In Vitro and in Vivo Data for Selected Compounds

			antiseizure DBA/2 mouse model		
compd	$^{45}Ca^{2+}$ flux IC_{50}, μM ± SEM[a]	K_i (nM) vs [^{3}H]MK-801 ± SEM[a]	% inhibition @ 20 mg/kg	% inhibition @ 10 mg/kg	% inhibition
8b	ND[b]	6116 ± 210	0	ND	
9b	0.39 ± 0.15	35140 ± 5070	ND	84	75 @ 4 mg/kg 41 @ 2 mg/kg
9d	ND	13488 ± 658	58	ND	
10b	3.5 ± 0.5	4410 ± 150	2	ND	
14b	0.9 (n = 1)	3840 ± 680	80	22	
18b	ND	4330 ± 210	69	ND	
18d	2.5 ± 0.5	3335 ± 245	43	ND	
20b	2.4 ± 0.5	3694 ± 234	81	44	
(+)-MK 801	ND	1.45 ± 0.16	ND	ND	82 @ 0.5 mg/kg
CNS 1237	2.7 ± 0.4	2485 ± 198	21	ND	
lamotrigine	ND	ND	ND	71	
riluzole	ND	ND	ND	81	
lubeluzole	ND	ND	66	ND	

[a] Values are means of at least three separate determinations ± SEM unless otherwise indicated. [b] ND = not determined.

the view that inhibition of [^{14}C]guanidinium influx in CNaIIA-1 cell line is a valid model for the identification of anti-ischemic Na^+ channel blockers. The Na^+ channel blockade properties of the compounds were determined as IC_{50} values and are reported in Table 1.

The block of synaptosomal Ca^{2+} channels was determined by inhibition of the $^{45}Ca^{2+}$ flux into brain synaptosomes depolarized by elevated K^+ concentration according to a method adapted from Nachsen and Blaustein,[38] as previously described.[7b,9,39] The rapid component of $^{45}Ca^{2+}$ uptake measured by this procedure is mediated by presynaptic neuronal Ca^{2+} channels, most probably P-type[14a] (Table 2). Affinity for the NMDA receptor ion-channel site was measured by inhibition of the binding of [^{3}H]MK-801 to rat brain membrane suspension.[30] Relative affinities of compounds were determined as IC_{50} values from displacement curves, and the results are presented in Table 2.

In vivo efficacy was evaluated for compounds with IC_{50} values below 2 μM in the type IIA Na^+ channel assay by assessing their anticonvulsant effect in audiogenic DBA/2 mice (6.5−12 g, 20−23 days of age).[40] Convulsions were induced by exposure to a 45-s pure tone sound of 12 kHz and 120 dB, 30 min after injection of the drug or vehicle. Animals were monitored for characteristic responses during the observation period. The response was rated from 0 (no response) to 4 (full seizure response followed by respiratory arrest) and is expressed as a percentage of control value (Table 2).

Biological Results and Discussion

The biological evaluation of these rigid guanidine analogues was performed using the following screening tests: (a) in vitro functional antagonism studies to determine neuronal type IIA Na^+ channel blockade

properties, (b) $^{45}Ca^{2+}$ uptake assay to evaluate selectivity, (c) in vivo anticonvulsant activity, (d) NMDA receptor binding assay.

In Vitro Sodium Channel Blockade. Unsubstituted analogues were examined for their ability to inhibit [^{14}C]guanidinium influx through blockade of neuronal type IIA Na^+ channels. As can be seen from data presented in Table 1, the flexible *N*,*N*′-diarylguanidine **18a** and the restricted analogues aminoquinazoline **4**, aminoimidazolines **8a** and **9c**, and aminopyrimidazolidine **9a** interact poorly with neuronal Na^+ channels ($IC_{50} \geq 10\ \mu M$) compared with the reference compound (CNS 1237). Likewise, the "lockamers" **14a** and **16**, the flexible counterpart *N*-aryl-*N*-alkylguanidine **20a**, and compound **10a** showed minimal inhibition of [^{14}C]-guanidinium influx ($IC_{50} > 17\ \mu M$).

All flexible and semirigid *p*-alkyl- or *p*-alkoxy-substituted derivatives tested do however interact strongly with Na^+ channels with IC_{50} values varying across a wide range. Comparison of the Na^+ channel binding activities for homologous pairs of compounds (e.g., **8a** vs **8b**, **9a** vs **9b**, **9c** vs **9d**, **10a** vs **10b**, **14a** vs **14b**) in Table 1 reveals that para-substituted compounds are consistently more potent. These results are in agreement with the SAR previously established for the flexible guanidines.[20,21] Comparison of the potencies of the various dialkyl-substituted "lockamers" showed the superiority of the aminopyrimidazoline **9b** and aminoimidazoline **9d** for neuronal Na^+ channel blockade.

Compound **3c**, locked in an AA^+ conformation, and **10b**, locked in an "AA^+-like" conformation ($IC_{50} = 2.9$ and 1.8 μM, respectively), have equal or slightly lower potency than the flexible analogues **18c** and **20b** ($IC_{50} = 3.28$ and 0.62 μM, respectively). These results tend to indicate that locking into an AA^+ or "AA^+-like" conformation has apparently a minimal effect on the ability of the disubstituted guanidinium cation to block neuronal Na^+ channels.

Compound **8b**, an AA^+, AS^+ restricted analogue, and **14b**, which mimics the AS^+ conformation, are slightly more potent than the AA^+ "lockamers" described above ($IC_{50} = 0.78$ and 0.46 mM, respectively), but these two compounds have a 10-fold lower potency than compounds **9b**,**d** ($IC_{50} = 0.06\ \mu M$) which are locked in an SS^+ conformation. Compounds **9b**,**d** display unprecedented potency for lipophilic guanidines, approaching the potency of tetrodotoxin in this assay ($IC_{50} = 0.004\ \mu M$), and are, to our knowledge, superior to previously reported synthetic Na^+ channel blockers. To prove the critical importance of the SS^+ conformation for the activity measured with **9b**, we tested compound **18d**, a tetrasubstituted guanidine which is the corresponding flexible analogue of **9d**, and **18b**, the non-N-methylated analogue. Compounds **18b**,**d** were found to be of average potency as blockers of [^{14}C]guanidinium influx ($IC_{50} = 0.8$ and 1 μM, respectively) compared to **9b**,**d**, demonstrating that the two- or three-methylene tether, bridging the nitrogen atoms, is not intrinsically responsible for the high activity of **9b**,**d** and that methylation of the two aryl-substituted nitrogen atoms, which results in the loss of two potential hydrogen bonds, has no effect on the ability of the *N*,*N*′-diphenylguanidinium to interact with the ion-channel site.

Taken together, these results suggest that spatial disposition of the pharmacophoric elements (aromatic rings and cationic center) achieved with these imidazoline- and pyrimidazoline-type scaffolds (**9b**,**d**) produces in this series of "lockamers" the best fit for blocking the ion-channel site. The lower activity of the flexible parent compound **18d** can be explained in terms of the energetic accessibility of this compound to alternate conformations (AA^+, AS^+) of lesser affinity. However, the relatively high affinity of compounds **8b** and **14b**, for which accessible conformations are of the types AA^+, AS^+ and "AS^+-like", respectively, indicates that these conformations contribute as well to the Na^+ channel activity of these compounds. The moderate activity of the two AA^+-based "lockamers" **3c** and **10b** suggests that AA^+ conformations contribute less to the blockade but still retain significant activity. With these results, the order of importance of the three types of conformations of diarylguanidines for neuronal type IIA Na^+ channel blockade can be proposed to be $SS^+ \gg AS^+ > AA^+$.

In Vitro Calcium Channel Blockade. To determine whether the semirigid Na^+ channel blockers identified above displayed a different selectivity for neuronal type IIA Na^+ channels over neuronal Ca^+ channels, selected compounds were tested in a synaptosomal $^{45}Ca^{2+}$ flux assay. Results in Table 2 show that compound **9b** is a potent blocker of neuronal Ca^{2+} channel with an $IC_{50} = 0.39\ \mu M$, which is 6 times lower than that of the flexible parent analogue **18d** ($IC_{50} = 2.5\ \mu M$); the ratio for these two compounds was 17 for neuronal Na^+ channel blockade. Comparison of selectivity for neuronal Na^+ vs Ca^{2+} channels shows a 3-fold improvement for **9b** compared to **18d** and CNS 1237. The rigid compounds **10b** and **14b** retain some activity ($IC_{50} = 3.5$ and 0.9 μM, respectively). These data indicate that rigidification does not well-separate neuronal Na^+ and Ca^{2+} channel blockade properties in this class of compounds. The high degree of structural homology between these types of voltage-activated ion channels could explain the difficulty to develop small molecules with channel-specific blocking properties.[41]

In Vivo Activity in the DBA/2 Mouse. The most potent semirigid Na^+ channel blockers along with the flexible analogues were evaluated for in vivo anticonvulsant activity in the DBA/2 mouse model. This test was chosen as the first in vivo model in our screening paradigm for neurotherapeutic agents because it provided an excellent tool for the rapid evaluation of central activity relevant to a Na^+ channel blockade mechanism.[42]

Compound **9b**, the ion-channel blocker endowed with the highest in vitro activity, was also found to be the most potent compound in vivo, showing considerable anticonvulsant activity when tested according to the general procedure described above, in the range of doses between 2 and 10 mg/kg (75% at 4 mg/kg) (Table 2). The semirigid compound **14b** ("AS^+-like") and the corresponding flexible analogue **20b**, which were nearly equipotent in vitro, showed good in vivo activity at 20 mg/kg, but the activity dropped sharply at 10 mg/kg. Compound **9d** (58% at 20 mg/kg) was found to be much less active than the six-membered ring analogue **9b**. Flexible analogues **18b**,**d** were moderately active at 20

mg/kg. Although compounds **8b** and **10b** both had potent in vitro activity (IC_{50} < 1.8 μM), they were both found to be inactive at the 20 mg/kg dose. Reference compounds lamotrigine and riluzole were found to have similar activity at 10 mg/kg to that of lead compound **9b**.

Within this small subset of seven compounds, in vivo data correlate reasonably well with in vitro results for four compounds but does not for the three imidazoline-based derivatives (**8b**, **9d**, and **10b**). The explanation for the total lack of activity of the two Na^+ channel blockers (**8b** and **10b**) at doses tested and the weak activity of **9d** is unknown, but it may arise from factors such as differences in the metabolism or distribution of the compounds and, in particular, access to the brain compared to the flexible parent compounds. However, the exceptional in vivo activity of **9b** is consistent with the much greater in vitro potency of this SS^+ "lockamer" in both the Na^+ and Ca^{2+} assays relative to the flexible molecules and other types of restricted analogues. Additionally, this assay was instrumental in identifying, among our in vitro leads, a compound family with CNS permeability for further in vivo studies.

NMDA Receptor Binding Studies. Many *N*,*N*′-diphenylguanidines have been reported in earlier studies[43] to be NMDA receptor antagonists. This class of compounds is known to suppress audiogenic seizures in the DBA/2 mouse.[44] It was therefore necessary to investigate a plausible cross-affinity of our Na^+ channel blockers with the NMDA receptor ion-channel site. In vitro radioligand binding experiments, using [^{3}H]MK-801 and rat brain membrane suspensions, were performed on the set of compounds which had demonstrated in vivo efficacy in the DBA/2 mouse model. The results presented in Table 2 indicate that these compounds have negligible affinity for the NMDA receptor ion-channel site. Therefore, we can rule out the possibility that the in vivo activity observed for these compounds was in part due to an NMDA receptor-mediated mechanism.

Physicochemical Studies. Passive diffusion of ionizable drugs through biological membranes such as the blood−brain barrier has been shown to correlate with lipophilicity at physiological pH (log $D_{7.4}$, D = octanol/water partition coefficient)[45,46] which, in turn, is a function of both inherent lipophilicity, log P, and the pK_a. Since introduction of a guanidine functionality into a rigid framework might alter the pK_a as well as the log P, pK_a and log $D_{7.4}$ values were measured for cyclic guanidine **9b** and the corresponding acyclic compound **18d**. The pK_a values of **9b** and **18d** were found to be ≥ 13.3 and 11.00, respectively. These results indicate that cyclization into a six-membered ring increases the basicity of the guanidine moiety and that the proportion of unprotonated **9b** is negligible at physiological pH. The latter result is a strong argument to support our hypothesis that the guanidinium ion is indeed the bioactive species.

However, assuming that active transport is not involved in this case, the potent in vivo activity of **9b** is difficult to reconcile with the generally held belief that charged molecules cannot effectively penetrate the blood−brain barrier. Under conditions approximating physiological salt and ionic strength (15 mM Hepes, 0.135 M NaCl), the log $D_{7.4}$ value for **9b** is 2.7, which is in the range considered optimal for blood−brain barrier penetration.[45,46] Since there is negligible free base present at physiological pH, it seems reasonable to conclude that uptake of **9b** by passive diffusion must be as the protonated species. This is supported by the constant log D observed below pH 9 (Figure 3), which is characteristic of partitioning of the protonated species as an ion pair,[47−50] presumably with chloride as the counterion. Experiments using a variety of other counterions have provided further evidence for ion-pair partitioning of **9b** between octanol and buffer,[51] and an effect of counterions on uptake into CACO-2 cell monolayers has also been observed for a diarylguanidine.[52] Ion pairing has also been implicated in GI absorption[53,54] and has been employed successfully in QSAR.[55] However, ion-pairing interactions with phospholipid headgroups in the lipid bilayer may have a strong influence on membrane uptake as well.[56]

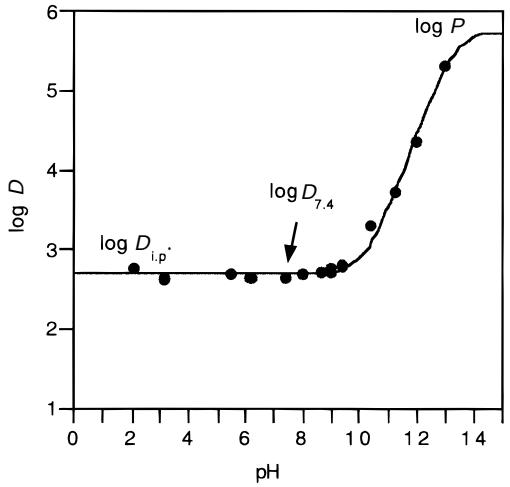

Figure 3. Dependence of log D of **9b** on pH. Solid line represents a 3-parameter fit of data (eq 1 in the Experimental Section) which includes the contributions of both the free base (B) and ion pair (BH^+Cl^-) to log D (log D_{ip} = log D of ion pair).

Conclusion

In conclusion, we have described a conformationally guided design strategy for a series of semirigid guanidino derivatives together with their chemical synthesis and pharmacological evaluation as neuronal Na^+ and Ca^{2+} channel blockers. Of the cyclic guanidines studied, "lockamers" **9b**,**d** demonstrated highly enhanced potency at blocking neuronal type IIA Na^+ channels, relative to flexible analogues and all other semirigid compounds synthesized. The lead compound that we identified met our design goal of creating a more potent Na^+ channel blocker, but it did not exhibit high selectivity for neuronal Na^+ versus Ca^{2+} channels.

These results lead us to postulate that the SS^+ conformation of the guanidine derivatives is of major importance for Na^+ and Ca^{2+} ion-channel blockade. These findings also suggest that if all these compounds have a common binding site(s) on the neuronal Na^+ channel, then such a site appears rather promiscuous in accommodating compounds with different rotameric orientations and is probably an amphipathic site with a deep hydrophobic pocket. The observation that increased lipophilicity at the para position of both aro-

matic rings is a major contributing factor to the ion-channel blockade is consistent with such a hypothesis.

In regard to the inhibition of seizures in the DBA/2 mouse, the good relationship between activity in this model and in vitro results, except for the three imidazoline-based "lockamers", validated our in vitro assay and enabled us to identify compound **9b** as the most active analogue in vivo in the DBA/2 mouse. Finally, the pyrimidazoline- and imidazoline-based "lockamers" **9a**−**d** provided important information on the geometrical parameters implicated in Na^+ channel blockade from which alternative spatial arrangements can be derived. Moreover, with this molecular scaffold a new class of neuronal mixed Na^+ and Ca^{2+} channel blockers with potent in vivo activity has been discovered, and further studies are in progress to evaluate members of this compound class for their potential as novel neurotherapeutics.

Experimental Section

Chemistry. General. Proton nuclear magnetic resonance spectroscopy was performed on a Varian GEMINI spectrometer (300 MHz), and data are reported as follows: chemical shift in ppm from internal standard on δ scale, multiplicity (b = broad, s = singlet, d = doublet, t = triplet, q = quadruplet, m = multiplet), and coupling constants (hertz). Infrared spectra were recorded on a Perkin-Elmer 1420 spectrometer. Chemical-ionization (CI) mass spectrometry was performed on a Finnegan 4500SQ spectrometer with NH_3 as reagent gas. All new compounds were either analyzed by C, H, and N elemental analysis (Galbraith Laboratories, Knoxville, TN, or Oneida Research, Whitesboro, NY) or characterized by exact mass determination for compounds which were not within ±0.4% of calculated value. Electron-impact (EI) high-resolution mass spectra (HRMS) were recorded on a Finnegan MAT 90 spectrometer. Compounds for which exact mass was employed were further analyzed by HPLC for homogeneity. HPLC purity analyses were carried out on a Beckman 126 gradient system with UV detection at 220 nm using a Beckman Ultrasphere ODS column (5 mm, 4.6 × 250 mm). The mobile phase was a linear 30-min gradient of 2−98% CH_3CN in H_2O (0.1% TFA) with a flow rate of 1 mL/min. Thin-layer chromatography (TLC) was performed on Merck silica gel 60 F_{254} precoated aluminum sheets (0.2 mm). Guanidines were visualized on TLC sheets with 254-nm UV light or as a blue spot with bromocresol green spray reagent (Aldrich Chemical Co). Column chromatography was performed with Merck silica gel 60 (230−400 mesh) as described by Still et al.[57] Melting points were determined in open capillary tubes on a Thomas-Hoover apparatus and are uncorrected.

Materials. Reagents were used as supplied from commercial sources. 4,4′-(Pentamethylenedioxy)bis(nitrobenzene) (**1**), 2-phenylquinoline **(12a**), 5,6,11,12-tetrahydodibenz[*b*,*f*]-azocine hydrochloride **(15**), and *N*-phenylethylenediamine (**7a**) were obtained from Aldrich Chemical Co. (Milwaukee, WI). Anhydrous quality (Sure/Seal) solvents (THF, ether, chlorobenzene) supplied by Aldrich Chemical Co. were used; all others solvents were reagent grade. Reactions involving organometallic reagents were run under an argon atmosphere.

9,15-Dioxa-2,4-diazatricyclo[14.2.2.2^{5,8}]docosa-2,5,7, 16,18,19,21-hepten-3-amine Hydrobromide (3c). To a solution of **1** (2.2 g, 6.3 mmol) in 170 mL of ethanol was added palladium on activated carbon (10%) (500 mg), and the suspension was hydrogenated with shaking at 50 psi for 16 h. The catalyst was filtered off on a bed of Celite and washed with 50 mL of ethanol, and the filtrates were combined. An aliquot was withdrawn and concentrated to characterize 4,4′-(pentamethylenedioxy)bis(aniline) (**2**): ^{1}H NMR ($CDCl_3$) δ 6.78 (s, 8H, Ar), 3.9 (t, J = 7 Hz, 4H, CH_2), 1.8 (m, 4H, CH_2), 1.6 (m, 2H, CH_2).

To the above ethanolic solution was added in ethanol (20 mL) cyanogen bromide (630 mg, 6 mmol), and the reaction mixture was stirred at room temperature overnight; 750 mL of ethanol was added and the solution heated at 90 °C for 6 h. Ethanol was evaporated, and the crude mixture obtained was purified on silica gel column with chloroform/methanol (9:1) as eluent to give **3c** (250 mg, 13%) as a white solid: mp 208−211 °C; ^{1}H NMR (CD_3OD) δ 6.72 (d, J = 7 Hz, 4H, Ar), 6.55 (d, J = 7 Hz, 4H, Ar), 4.1 (t, J = 6 Hz, 4H, CH_2), 1.6 (m, 4H, CH_2), 1.35 (m, 2H, CH_2); CI-MS 312 [MH^+]. Anal. ($C_{18}H_{21}N_3O_2$·HBr) H, N; C: calcd, 55.12; found, 55.95. HR-MS calcd for $C_{18}H_{21}N_3O_2$: [$M^{\bullet+}$] 311.1634. Found: 311.1638. HPLC: 95% pure.

***N*-(4-*sec*-Butylphenyl)ethylenediamine (7b).** This procedure illustrates the general method for the preparation of **7b**−**d**. The formaldehyde sodium bisulfite addition compound used in the preparation of **7b** was replaced with benzaldehyde and sodium bisulfite for **7c**,**d**. 4-*sec*-Butylaniline (5.6 g, 37 mmol) was added to 25% aqueous acetic acid (200 mL) containing formaldehyde sodium bisulfite addition compound (15 g, 110 mmol), and the resulting mixture was stirred at 60 °C for 1 h. The solution was then cooled to room temperature, and potassium cyanide (7.2 g, 110 mmol) was added (pH = 5). The mixture was stirred for 3 days at 60 °C, cooled, and concentrated to 60 mL. This solution was then placed in an ice bath until precipitation of a white solid occurred. This solid was filtered off and washed with water to give *N*-(4-*sec*-butylphenyl)glycine nitrile (**6b**) (5.8 g, 82%): ^{1}H NMR (CD_3-OD) δ 7.1 (m, 2H, Ar), 6.7 (m, 2H, Ar), 4.0 (s, 2H, CH_2), 2.6 (m, J = 7 Hz, 1H, *sec*-butyl-H), 1.6 (q, J = 7 Hz, 2H, *sec*-butyl-CH_2), 1.25 (d, J = 7 Hz, 3H, *sec*-butyl-CH_3), 0.85 (t, J = 7 Hz, 3H, *sec*-butyl-CH_3); CI-MS 206 [MNH_4^+].

This material (5.7 g, 30 mmol) was then dissolved in 2 N methanolic ammonia (120 mL), treated with Raney nickel (2 g), and hydrogenated under 50 psi at room temperature overnight. The catalyst was filtered off on a bed of Celite and washed with methanol. The combined filtrates were concentrated in vacuo, and the crude mixture obtained was purified on silica gel with chloroform/methanol (9:1) as eluent to give **7b** (3.6 g, 60% yield) as an oil: ^{1}H NMR (CD_3OD) δ 7.0 (m, 2H, Ar), 6.7 (m, 2H, Ar), 3.2 (t, J = 5 Hz, 2H, CH_2), 2.9 (t, J = 5 Hz, 2H, CH_2), 2.5 (m, J = 7 Hz, 1H, *sec*-butyl-H), 1.55 (q, J = 7 Hz, 2H, *sec*-butyl-CH_2), 1.2 (d, J = 7 Hz, 3H, *sec*-butyl-CH_3), 0.85 (t, J = 7 Hz, 3H, *sec*-butyl-CH_3); CI-MS 193 [MH^+].

Phenyl(1-phenyl-4,5-dihydro-1*H*-imidazol-2-yl)amine Mesylate (8a). A solution of *N*-phenylethylenediamine (**7a**) (2.0 g, 15 mmol) in 30 mL of ethanol was stirred while carbon disulfide (0.9 mL, 15 mmol) was added dropwise, and the mixture was heated at 50 °C for 3 h. The solution was cooled, and the precipitated *N*-phenylimidazolidine-2-thione was collected (2.27 g, 87%). MeI (1.25 mL, 20 mmol) was added dropwise to a suspension of the above solid (1.54 g, 8.64 mmol) in 20 mL of methanol and the reaction mixture heated at 60 °C for 3 h. The solution obtained was concentrated on a rotary evaporator to an oil, and excess aniline **5a** (2 mL) was added. The mixture was then heated at 90 °C for 2 h. Excess aniline was removed under high vacuum, and 0.1 N aqueous NaOH was added. This solution was extracted with EtOAc three times, and the combined EtOAC extracts were washed with brine and concentrated to dryness. The crude mixture obtained was purified on a silica gel column using chloroform/methanol (9:1) as eluent. The fractions containing the product were combined and concentrated to yield the free base of **8a** (0.69 g). The concentrate was dissolved in Et_2O, and methanesulfonic acid (0.18 mL) was added to give **8a** (0.75 g, 26% from the thione) as a white solid: mp 180−182 °C; ^{1}H NMR (CD_3OD) δ 7.60−7.30 (m, ArH, 10H), 4.21 (dd, J = 10 Hz, 2H, CH_2), 3.83 (dd, J = 10 Hz, 2H, CH_2), 2.68 (s, CH_3SO_3H, 3H); CI-MS 238 [MH^+]. Anal. ($C_{15}H_{15}N_3$·CH_3SO_3H) C, H, N.

(4-*sec*-Butylphenyl)(1-(4-*sec*-butylphenyl)-4,5-dihydro-1*H*-imidazol-2-yl)amine Mesylate (8b). Using the same procedure as described for the preparation of **8a**, compound **8b** was prepared from **7b** and isolated as a white solid: mp 98−99 °C (35% yield from **7b**); ^{1}H NMR ($CDCl_3$) δ 7.0 (s, 4H, Ar), 6.88 (s, 4H, Ar), 4.15 (t, J = 8 Hz, 2H, CH_2), 3.95 (t, J =

8 Hz, 2H, CH_2), 2.70 (s, 3H, CH_3SO_3H), 2.4 (m, 2H, *sec*-butyl-H), 1.45 (m, 4H, *sec*-butyl-CH_2), 1.1 (2d, $J = 7$ Hz, 6H, *sec*-butyl-CH_3), 0.70 (t, $J = 7$ Hz, 6H, *sec*-butyl-CH_3); CI-MS 349 [MH^+]. Anal. ($C_{23}H_{31}N_3 \cdot CH_3SO_3H$) C, H, N.

1,3-Diphenyltetrahydropyrimidin-2-ylidenamine Hydrobromide (9a). *N*,*N*′-diphenyl-propane[58] (0.83 g, 3.67 mmol) and cyanogen bromide (0.34 g, 3.08 mmol) were mixed together, and the paste obtained was heated to 110 °C for 30 min and stirred frequently with a spatula. The fused reaction mixture was allowed to cool to room temperature and the resulting solid dissolved in 2 mL of $CHCl_3$. This crude solution was purified on a silica gel column with $CHCl_3$/MeOH (20:1) as eluent. The fractions which contained the product were collected and concentrated to yield a light-brown oil. This oil was dissolved in 10 mL of Et_2O, and after 0.5 h of stirring, a white solid precipitated out. This solid was collected by filtration, washed with Et_2O, and dried under vacuum to give **9a** (0.67 g, 55%) as a white solid: mp 210−211 °C; ^{1}H NMR (CD_3OD) δ 7.65−7.45 (m, ArH, 10H), 3.84 (t, $J = 8$ Hz, 4H, NCH_2), 2.40 (m, CH_2, 2H); EI-MS: *m*/*z* 251 [$M^{\bullet+}$] ($C_{16}H_{17}N_3$). Anal. ($C_{16}H_{17}N_3 \cdot HBr$) C, H, N.

1,3-Bis(4-*sec*-butylphenyl)tetrahydropyrimidin-2-ylidenamine Hydrobromide (9b). Compound **9b** was prepared according to the same procedure as described for **9a** (yield = 65%, last step): white solid, mp > 250 °C; ^{1}H NMR ($CDCl_3$) δ 7.68 (d, $J = 7$ Hz, 4H, Ar), 7.30 (d, $J = 7$ Hz, 4H, Ar), 4.10 (t, $J = 8$ Hz, 4H, NCH_2), 2.65 (m, $J = 6$ Hz, 2H, *sec*-butyl-H), 2.4 (m, 2H, CH_2), 1.60 (m, 4H, *sec*-butyl-CH_2), 1.25 (d, $J = 7$ Hz, 6H, *sec*-butyl-CH_3), 0.80 (t, $J = 7$ Hz, 6H, *sec*-butyl-CH_3); EI-MS *m*/*z* 362 [$M^{\bullet+}$]. Anal. ($C_{24}H_{33}N_3 \cdot HBr \cdot 0.25H_2O$) C, N, H.

1,3-Diphenyl-4,5-dihydroimidazol-2-ylamine Hydrobromide (9c). Compound **9c** was prepared according to the same procedure as described for **9a** (yield = 51%, last step): white solid, mp 239−240 °C; ^{1}H NMR (CD_3OD) δ 7.35−7.65 (m, 10H, ArH), 4.22 (s, 4H, NCH_2); CI-MS 238 [$M^{\bullet+}$]. Anal. ($C_{15}H_{15}N_3 \cdot HBr$) C, N, H.

1,3-Bis(4-*sec*-butylphenyl)-4,5-dihydroimidazol-2-ylamine Hydrobromide (9d). Compound **9d** was prepared according to the same procedure as described for **9a** (yield = 46%, last step): white solid, mp 229−230 °C; ^{1}H NMR (CD_3OD) δ 7.35−7.50 (m, 8H, ArH), 4.19 (s, 4H, NCH_2), 2.50−2.80 (m, 2H, 2CH), 1.60−1.70 (m, 4H, *sec*-butyl-CH_2), 1.26 (d, $J = 7$ Hz, 6H, *sec*-butyl-CH_3), 0.86 (t, $J = 7$ Hz, 6H, *sec*-butyl-CH_3). EI-MS *m*/*z* 349 [$M^{\bullet+}$]. Anal. ($C_{23}H_{31}N_3 \cdot HBr$) C,N,H.

(*R*,*S*)-2-Amino-4,5-dihydro-1,5-diphenyl-1*H*-imidazole Hydrobromide (10a). The diamine **7c** (334 mg, 1.57 mmol) was dissolved in 5 mL of ethanol, and cyanogen bromide (1.73 mmol, 189 mg) was added at 0 °C with stirring. The reaction mixture was heated to 85 °C for 1.5 h. The reaction mixture was concentrated to about 2 mL to which was added 20 mL of diethyl ether, and the mixture was stirred for 10 min. Compound **10a** precipitated as a white solid (414 mg, 83%): mp 232−234 °C; ^{1}H NMR ($CDCl_3$) δ 7.45−7.00 (m, ArH, 10H), 5.27 (q, $J = 10$, 8 Hz, 1H, CH), 4.31 (t, $J = 10$ Hz, 1H, CH_2), 3.86 (q, $J = 10$, 8 Hz, 1H, CH_2); CI-MS 238 [MH^+]. Anal. ($C_{15}H_{15}N_3 \cdot HBr$) C, H, N.

(*R*,*S*)-2-Amino-4,5-dihydro-1-(4′-*sec*-butylphenyl)-5-(4′-isopropylphenyl)-1*H*-imidazole Hydrobromide (10b). Using the same procedure as described for the preparation of **10a**, compound **10b** was prepared from **7d**. The yield of **10b** was 77%: white solid, mp 188−189 °C; ^{1}H NMR ($CDCl_3$) δ 7.40−6.65 (m, 8H, Ar), 5.20 and 5.05 (m, 1H, CH−N), 4.2 and 3.9 (m, 1H, CH−N), 3.7 and 3.2 (m, 1H, CH−N), 2.85 (m, 1H, isopropyl-H), 2.55 and 2.25 (m, 1H, *sec*-butyl-H), 1.55 and 1.35 (m, 2H, *sec*-butyl-CH_2), 1.2 and 0.95 (m, 9H, isopropyl-CH_3, *sec*-butyl-CH_3), 0.75 and 0.65 (m, 3 H, *sec*-butyl-CH_3); EI-MS [$M^{\bullet+}$] 335. Anal. ($C_{22}H_{29}N_3 \cdot HBr$) C, H, N.

2-(4-*tert*-Butylphenyl)-6-isopropylquinoline (12b). To a cooled (ice bath) 2 M diethyl ether solution of 4-*tert*-butylphenylmagnesium bromide (15 mL, 0.03 mol) was added dropwise under argon 15 mL of a tetrahydrofuran solution of 6-isopropylquinoline (5.13 g, 0.03 mol). The resulting mixture was refluxed for 5 h, stirred at room temperature for 12 h, and quenched with water. The yellow precipitate obtained was then filtered and washed with hexane. Crystallization in hexane/chloroform (40:1) yielded **12b** (3.7 g, 40%): ^{1}H NMR ($CDCl_3$) δ 8.2 (m, 4H, Ar), 7.84 (m, 1H, Ar), 7.60 (m, 4H, Ar), 3.12 (m, 1H, isopropyl), 1.4 (m, 15H, isopropyl-CH_3, *tert*-butyl-CH_3); CI-MS 304 [MH^+].

(*R*,*S*)-2-Phenyl-1,2,3,4-tetrahydroquinoline Hydrochloride (13a). To a solution of **12a** (1 g, 4.8 mmol) in 100 mL of methanol was added platinum(IV) oxide (200 mg, 0.8 mmol), and the suspension was hydrogenated with shaking at 50 psi for 12 h. The catalyst was filtered off on a bed of Celite and washed with methanol. 20 mL of 1 N HCl in ethyl ether was added to the combined filtrates which were then concentrated to yield **13a** (0.38 g, 31%): ^{1}H NMR ($CDCl_3$) δ 7.6 (m, 4H, Ar), 7.40 (m, 4H, Ar), 7.10 (m, 1H, Ar), 4.4 (dd, $J = 2.5$, 10 Hz, 1H, CH), 2.9 (m, 2H, CH_2), 2.6 (m, 1H, CH_2), 2.35 (m, 1H, CH_2); CI-MS 209 [MH^+].

(*R*,*S*)-2-(4-*tert*-Butylphenyl)-6-isopropyl-1,2,3,4-tetrahydroquinoline Hydrochloride (13b). Using the same procedure as described for the preparation of **13a**, compound **13b** was prepared from **12b**. The yield of **13b** was 30%: ^{1}H NMR ($CDCl_3$) δ 7.38 (m, 4H, Ar), 6.90 (m, 2H, Ar), 6.52 (m, 1H, Ar), 4.39 (dd, $J = 2.5$, 10 Hz, 1H, CH), 2.85 (m, 3H, isopropyl-H, CH_2), 2.1 (m, 2H, CH_2), 1.2 (m, 15H, isopropyl-CH_3, *tert*-butyl-CH_3); CI-MS 308 [MH^+].

(*R*,*S*)-1-Carboximidamido-2-phenyl-1,2,3,4-tetrahydroquinoline Hydrochloride (14a). To a solution of **13a** (300 mg, 1.2 mmol) in 20 mL of ethanol was added cyanamide (335 mg, 8 mmol), and the mixture was heated to reflux for 2 days. The solvent was evaporated, water was added, and the product was extracted with ethyl acetate. The organic layer was separated, dried over Na_2SO_4, filtered, and concentrated. Purification of the crude mixture was achieved on silica gel with chloroform/methanol (9:1) as eluent. The solid obtained was washed successively with water and ethyl ether and dried in vacuo to give pure **14a** (80 mg, 23%) as a white solid: mp 202−204 °C; ^{1}H NMR ($CDCl_3$) δ 7.40 (m, 9H, ArH), 5.02 (dd, $J = 6$, 12 Hz, 1H, CH), 2.80 (m, 2H, CH_2), 1.6−1.9 (complex band, 2H, CH_2); CI-MS 252 [MH^+]. Anal. ($C_{16}H_{17}N_3 \cdot HCl$) C, H, N.

(*R*,*S*)-1-Carboximidamido-2-(4-*tert*-butylphenyl)-6-isopropyl-1,2,3,4-tetrahydroquinoline Hydrochloride (14b). Using the same procedure as described for the preparation of **14a**, compound **14b** was prepared from **13b**. The yield of **14b** was 25% (white solid): mp 208−210 °C; ^{1}H NMR (CD_3OD) δ 7.40 (m, 4H, ArH), 7.20 (m, 3H, ArH), 5.30 (m, CH, 1H), 2.90 (m, $J = 6$ Hz, 1H, isopropyl), 2.70 (m, 3H, CH_2), 1.9 (m, 1H, CH_2), 1.2 (m, 15H, isopropyl-CH_3, *tert*-butyl-CH_3); CI-MS 350 [MH^+]. Anal. ($C_{23}H_{31}N_3 \cdot HCl \cdot H_2O$) C, H, N.

5-Carboximidamido-5,6,11,12-tetrahydrodibenz[*b*,*f*]-azocine Hydrochloride (16). Using the same procedure as described for the preparation of **14a**, compound **16** was prepared from **15**. The yield of **16** was 58% (white solid): mp 238−240 °C; ^{1}H NMR (CD_3OD) δ 7.10 (m, 8H, ArH), 5.28 (d, $J = 13$ Hz, 1H, N−CH), 4.6 (d, 1H, $J = 13$ Hz, N−CH), 3.20 (m, 2H, CH_2), 3.0 (m, 2H, CH_2); CI-MS 252 [MH^+]. Anal. ($C_{16}H_{17}N_3 \cdot HCl$) C, H, N.

***N*,*N*′-Diphenylguanidine Hydrobromide (18a).** This procedure illustrates the general method for the preparation of **18a**−**c**. Cyanogen bromide (565 mg, 5.3 mmol) was added slowly in portions to a stirred solution of aniline **17a** (1 mL, 10.7 mmol) at 0 °C in ethanol (3 mL). After the exothermic reaction subsided, the reaction mixture was allowed to warm to room temperature and then heated at 100 °C until the solvent has evaporated (1.5 h). The fused reaction mixture was allowed to cool to room temperature, and the resulting solid was triturated in Et_2O (20 mL) until a fine suspension was obtained. This suspension was stirred for 2 h and filtered, and the solid obtained was washed with Et_2O twice to yield pure **18a** (1.52 g, 97%) as a white solid: mp 158−160 °C; ^{1}H NMR ($CDCl_3$) δ 7.20 (m, 10H, ArH); CI-MS 212 [MH^+]. Anal. ($C_{13}H_{13}N_3 \cdot HBr$) C, H, N.

***N*,*N*′-Bis(4-*sec*-butylphenyl)-*N*,*N*′-dimethylguanidine Hydrochloride (18d).** A solution of cyanogen bromide (2.2

g, 20 mmol) in Et_2O (25 mL) was added slowly to a stirred solution of 4-*sec*-butylaniline (5 g, 30 mmol) in Et_2O (50 mL), and stirring continued at room temperature overnight. A white precipitate of 4-*sec*-butylaniline hydrobromide (3.4 g) was filtered off, and the filtrate was washed with Et_2O. Evaporation of the ether wash afforded 4-*sec*-butylcyanamide (2.9 g, 83%) as a thick liquid: IR (film) 2225 cm^{-1}. A solution of the cyanamide (2.3 g, 13.5 mmol) and sodium hydride (0.9 g, 27 mmol, prewashed twice with hexanes) in anhydrous THF (10 mL) was heated at 80 °C for 2 h. After the reaction mixture was allowed to cool to room temperature, methyl iodide (7.05 g, 50 mmol) was added, and stirring continued at room temperature for 2 h. Methanol (15 mL) followed by water (35 mL) were added, and the reaction mixture was extracted with CH_2Cl_2 (2 × 40 mL). Concentration of the organic layer followed by flash chromatography on SiO_2 afforded *N*-(4-*sec*-butylphenyl)-*N*-methylcyanamide (**17e**) (2.0 g, 80%) as a colorless liquid: IR (film) 2200, 3400 cm^{-1}.

To a solution of **17e** (500 mg, 2.6 mmol) in toluene (15 mL) was added aluminum chloride (390 mg, 2.9 mmol) and the reaction mixture heated to 100 °C until the catalyst dissolved. Then, the hydrochloride of *N*-methyl-4-*sec*-butylaniline (**17d**)[31] (465 mg, 2.3 mmol) was added in chlorobenzene (5 mL) at room temperature, and the mixture was heated at 100 °C for 5 h. The solution was cooled, diluted with chloroform, and washed with H_2O. Concentration of the organic layer followed by flash chromatography on SiO_2 with chloroform/methanol (10:1) as eluent afforded **18d** (350 mg, 38%) as a white-yellow hygroscopic solid: mp 65−66 °C; ^1H NMR (CD_3OD) δ 7.0 (d, J = 7 Hz, 4H, Ar), 6.80 (d, J = 7 Hz, 4H, Ar), 3.35 (s, 6H, N−CH_3), 2.5 (m, J = 6 Hz, 2H, *sec*-butyl-H), 1.55 (m, CH_2, 4H, *sec*-butyl-CH_2), 1.15 (d, J = 6 Hz, 6H, *sec*-butyl-CH_3), 0.80 (t, J = 6 Hz, 6H, *sec*-butyl-CH_3); EI-MS m/z 351 [$M^{\bullet+}$]. Anal. ($C_{23}H_{33}N_3$·HCl·1.75H_2O) C, H; N: calcd, 10.07; found, 11.27. HR-MS calcd for $C_{23}H_{33}N_3$: 351.2674. Found: 351.2660 [$M^{\bullet+}$]. HPLC: 95% pure.

***N*-Benzyl-*N*-phenylguanidine Hydrochloride (20a).** Benzyl bromide (5.13 g, 30 mmol) was slowly added to solution of aniline (2.79 g, 30 mmol) and Et_3N (4.55 g, 45 mmol) in 75 mL of CH_2Cl_2. The reaction mixture was protected from the light and stirred at room temperature overnight. The precipitate was filtered off, and the solvent was removed. The crude product obtained was purified on silica gel column with hexanes/CH_2Cl_2 (4:1 to 2:1). The fractions which contained the product were collected and concentrated. The yellow oil obtained was dissolved in Et_2O, and 50 mL of 1 M HCl in Et_2O was added. The precipitate was collected by filtration, washed with Et_2O, and dried under vacuum to yield **19a** (2.79 g, 42%) as a white solid: mp 205−207 °C; ^1H NMR ($CDCl_3$) δ 7.39−7.22 (m, 10H, ArH), 4.35 (s, 2H, ArCH_2); EI-MS m/z 183 [$M^{\bullet+}$].

To a solution of **19a** (2.79 g, 12.7 mmol) in 25 mL of CH_2Cl_2 was added cyanamide (3.20 g, 76.2 mmol), and the reaction mixture was refluxed for 12 h. The crude product obtained after evaporation of the solvent was purified on a silica gel column with chloroform/methanol (10:1) as eluent. The fractions collected containing the product were concentrated, and 150 mL of water was added; 1 N NaOH was added to this solution until pH = 14, and the product was extracted three times with CH_2Cl_2. The combined extracts were washed with water and brine and dried over $MgSO_4$. The free base obtained was then dissolved in Et_2O, 10 mL of 1 M HCl in Et_2O was added, and **20a** precipitated (1.10 g, 33% from **19a**) as a white solid: mp 251−252 °C; ^1H NMR (CD_3OD) δ 7.40−7.10 (m, 10H, Ar), 4.85 (s, 2H, CH_2); EI-MS m/z 225. Anal. ($C_{14}H_{15}N_3$·HCl) C, H, N.

***N*-(4-*sec*-Butylphenyl)-*N*-(4-*tert*-butylbenzyl)guanidine Mesylate (20b).** Using the same procedure as described for the preparation of **20a**, compound **20b** was prepared from **17b**. Methanesulfonic acid was used for the preparation of the salt of **20b**. The yield of **20b** was 79% from **19b**: white solid, mp 177−178 °C; ^1H NMR ($CDCl_3$) δ 7.12−7.40 (m, 8H, ArH), 4.95 (s, ArCH_2, 2H), 2.72 (s, 3H, CH_3SO_3H), 2.60 (m, J = 6 Hz, 1H, *sec*-butyl-H), 1.60 (m, CH_2, 2H, *sec*-butyl-CH_2), 1.30 (s, 9H, *tert*-butyl), 1.20 (d, J = 6 Hz, 3H, *sec*-butyl-CH_3), 0.80 (t, J = 6 Hz, 3H, *sec*-butyl-CH_3); EI-MS m/z 225. Anal. ($C_{22}H_{31}N_3$·CH_3SO_3H) C, H, N.

Pharmacology. In Vitro Experiments. Inhibition of Veratridine-Induced [^{14}C]Guanidinium Influx. Chinese hamster ovary cell lines (CNaIIA-1) that stably express the α-1 subunit of the mammalian type IIA neuronal sodium channel were used as a model system for our assays.[33] The CNaIIA-1 cells were cultured at 37 °C with 5% CO_2 in RPMI 1640 (MediaTech) supplemented with 5% fetal calf serum (Hyclone), 200 μg/mL G418 (Sigma), and 5.75 mg/mL proline (Sigma). EDTA-free trypsin (1:250; Sigma) was used to split the cells once a week, and cells were seeded at a density of 1 × 10^5/T75 flask (CoStar). For the flux assay, 96-well plates were seeded with 2 × 10^4 cells/well in 200 μL of culture media. Cells were routinely allowed to grow for 4−5 days in vitro before conducting an assay. Cell number was assessed by hemocytometry to be approximately 80 000 cells/well on the day of assay. The culture medium was changed every 3 days. Cells whose passage number exceeded 30 were not used. Cultures were rinsed three times with 200 μL of preincubation buffer (mM: KCl, 5.4; $MgSO_4$, 0.8; HEPES, 50; choline chloride, 130; guanidine HCl, 1.0; d-glucose, 5.5; BSA, 0.1 mg/mL; pH 7.4) and incubated with 200 μL of preincubation buffer at 37 °C for 10 min. A 96-channel manifold was used to vacuum-aspirate the buffer from the wells between rinses. Veratridine-induced [^{14}C]guanidinium flux was linear with time up to at least 1 h, and a robust signal (4−8-fold basal flux) was obtained following a 1-h incubation. Different concentrations of test compounds were prepared by serial dilution of a 200 μM stock solution in uptake buffer (preincubation buffer plus [^{14}C]guanidine·HCl and veratridine; final concentrations ranged from 0.001 to 25 μM for test compounds, 2.5 μCi/mL for [^{14}C]guanidine·HCl, and 200 μM for veratridine). The flux experiments were run in a 100-μL volume and were initiated by the addition of 50-μL aliquots of the above working stocks to an equal volume of preincubation buffer in the 96-well plates which were then incubated at room temperature for 1 h. The following controls were also conducted in each 96-well plate: basal flux (obtained in the absence of test compound and veratridine), veratridine-only-induced flux, and veratridine-induced fluxes in the presence of 10 μM tetrodotoxin (TTX), a measure of nonspecific flux; 10 mM stock solutions of test compounds were prepared by dissolving the appropriate amount of the salt of the compound to 100% DMSO. This was further diluted in uptake buffer to yield a 200 μM stock solution. Final assay concentrations of DMSO were <1%. A 200 mM working concentration of veratridine was prepared by dissolving it in 100% methanol. Final assay concentrations of methanol were 0.1%. The flux assay was terminated at the end of the incubation period by rinsing the 96-well plates three times (200 μL/well) with ice-cold wash buffer (mM: choline chloride, 163; $MgSO_4$, 1.8; $CaCl_2$, 1.8; HEPES, 5.0; BSA, 1.0 mg/mL). The remaining 50 μL of wash buffer in the wells (following rinsing) was vacuum-aspirated. Optiphase "HiSafe" (Wallac) scintillation fluid (100 μL) was then added to each well. The plates were sealed before shaking for 15 min. The plates were then allowed to sit for 45 min before counting in a 96-well Microbeta 1450 scintillation counter. Net veratridine-induced [^{14}C]guanidinium flux was determined for each concentration of each compound tested. Net flux is obtained by subtracting the nonspecific flux (flux in the presence of veratridine and TTX only) from the total flux (flux in the presence of veratridine only or veratridine and competing ligand). Results were plotted as percent inhibition of veratridine-induced [^{14}C]guanidinium uptake versus compound concentration for each compound tested, and IC_{50} values were determined by fitting the data to a nonlinear regression function.

Synaptosomal $^{45}Ca^{2+}$ Uptake. The protocol for this assay has been described earlier.[6b,9,39]

Radioligand Binding Assays. The protocol for this assay has been described earlier.[30]

In Vivo Experiments. Antiseizure DBA/2 Mouse Model. DBA/2 mice of either sex (Jackson Lab, ME; weight range 6.5−

12 g, 20−23 days of age) were placed individually in a glass jar (25-cm i.d.) and exposed to pure tone sound of 12 kHz and 120 dB. Animals were injected with the drugs or vehicle (0.3 M mannitol, administered by ip injection, in a volume of 10 mL/kg of body weigh) 30 min prior to exposure to the sound. The auditory stimulation was applied for 45 s or until respiratory arrest occurred. The apparatus used for sound generation consisted of a high-frequency driver, an amplifier, and a function generator. All experiments were proceeded in a fully blinded fashion and took place between 11 a.m. and 5 p.m. Animal response was scored as follows: 0 = no response; 1 = wild running; 2 = clonic seizures; 3 = tonic seizures; 4 = seizures resulting in respiratory arrest. The *N* for each dose was 10−13. The individual scores of animals in each treatment group were averaged to yield a mean response score (MRS) for the group. The percentage of response inhibition for each treatment group was calculated as follows: percentage response inhibition = (MRS control − MRS treatment)/MRS control × 100. The Jonckheere nonparametric trend test, one-sided, was used to determine the lowest effective dose in dose−response studies. Otherwise, the Kruskal−Wallis nonparametric test was used, with Dunn's post hoc test.

Molecular Mechanics Calculations. The molecular mechanics calculations have been carried out at the University of Toledo with the Macromodel 6.0[19a] software running on a Silicon Graphics workstation. In-solution modeling used the Generalized Born/Surface Area approximation of Still et al.[19b] as implemented in the software. The modified AMBER[19c] force field was applied with atomic charges and steric parameters taken from the program library. The dielectric constant for the electrostatic interactions of the solute atoms was set to unity, while the bulk permitivity values were accepted for both water and chloroform. Conformational analyses were carried out by performing multiconformational search in solution for compounds **3a**−**c**. Four, six, or eight bonds, each by steps of 60°, were independently rotated in the 0−360° range respectively for the $-Ph-O-(CH_2)_n-O-Ph-$ (n = 1, 3, 5) moieties. Restriction on the macrocycle of compounds **3a**−**c** was imposed by the distance requirement of 1.27−1.40 Å for the N−C+ bond. Rotamers that met the distance requirement were separately submitted to full geometry optimization. Multiconformational search for compound **18c** in the AA^+ conformation consisted of independent rotations of 60° about the $C_{Ar}-O$ and $O-CH_2$ bonds. Value ranges for the rotational angles ψ_1 and ψ_2 that minimize the AA^+ energy in water or chloroform are reported as follows: **3a** (121−124), **3b** (138−140), **3c** (144−148), **18c** (160−163).

pK_a Determination. The pK_a value of **9b** was determined by using log *D* vs pH measurement, and UV vs pH was used for **18d**. To the compound (0.2−1 mg) in a 20-mL scintillation vial were added preequilibrated octanol and buffer (15 mM HEPES/135 mM NaCl except for pH 2, where used or 15 mM sodium phosphate/135 mM NaCl). The ratio of buffer to octanol volumes was in the range of 1−5. The mixture was shaken at full speed with a Burrell Wrist-Action shaker (model 75) for 10 min at ambient temperature (23 ± 1 °C), and layers were carefully separated after centrifugation. After the pH of the aqueous layer was determined, an aliquot was acidified and the concentration was determined by reverse-phase HPLC. Chromatography was conducted on a Waters 616 system with UV detection using a Spherisorb CN column (3 μm, 4.6 × 150 mm) at ambient temperature. An isocratic mobile phase consisting of various ratios of AcCN and phosphate buffer (pH 3.5) was employed (flow rate = 1 mL/min). Solutions for standard curves were prepared in pH 2 Hepes buffer. The concentration in the organic layer was also determined, by UV absorbance in a spectrophotometer after dilution into 0.1 N HCl in EtOH. The log *D* was calculated from $\log(C_{oct}/C_{buf})$. The reported value is the average of results from three individual partition experiments.

Experimental log *D* vs pH data were interatively fit using the program KaleidaGraph (Abelbeck Software) to eq 1[47] to yield the pK_a value, log *P*, and log D_{ip}:

$$\log D = \log(10^{\log P} + 10^{(\log D_{ip} + pK_a - pH)}) - \log(1 + 10^{(pK_a - pH)}) \quad (1)$$

where

$$D = \frac{[BH^+]_{org} + [B]_{org}}{[BH^+]_{aq} + [B]_{aq}}, \quad P = \frac{[B]_{org}}{[B]_{aq}}, \quad D_{ip} = \frac{[BH^+]_{org}}{[BH^+]_{aq}}$$

In the case of **9b**, only a limiting value of the pK_a could be determined since log *P* cannot be accurately measured above pH 13.

The measurement of pK_a of **18d** was performed using the pH dependence of UV absorbance as described by Albert and Sergeant.[59] Measurements were obtained in 10 mM aqueous buffer.

Acknowledgment. We would like to express our thanks to Robert Egan for the synthesis of some intermediate chemicals, N. Laxma Reddy for the preparation of the first batch of compound **18b**, Bing Guan for the synthesis of a second batch of compound **4**, Kathleen J. Burke Howie for performing the NMDA binding assay, and Dr. William F. Holt.

Supporting Information Available: Listing of coordinates and energies for **3a**−**c** and **18c** in water and chloroform from molecular modeling study (11 pages). Ordering information is given on any current masthead page.

References

(1) (a) Catteral, A. W. Common Modes of Drug Action on Na^+ Channels: Local Anesthetics, Antiarrhythmics and Anticonvulsants. *Trends Pharm. Sci.* **1987**, *8*, 57−65. (b) Rogawski, M. A.; Porter, R. J. Antiepileptic Drugs: Pharmacological Mechanisms and Clinical Efficacy with Consideration of Promising Development Stage Compounds. *Pharmacol. Rev.* **1990**, *42*, 223−286.

(2) (a) Taylor, C. P. Voltage-gated Na^+ Channels as Targets for Anticonvulsant, Analgesis and Neuroprotective Drugs. *Curr. Pharm. Des.* **1996**, *2*, 375−388. (b) Taylor, C. P.; Narasimhan, L. S. Sodium Channels and Therapy of Central Nervous System Diseases. *Adv. Pharmacol.* **1997**, *39*, 47−98.

(3) Urenjak, J.; Obrenovitch, T. P. Pharmacological Modulation of Voltage-Gated Na^+ Channels: A Rational and Effective Strategy Against Ischemic Brain Damage. *Pharmacol. Rev.* **1996**, *48*, 21−67.

(4) Agrawal, S. K.; Fehlings, M. G. Mechanisms of Secondary Injury to Spinal Cord Axons In Vitro: Role of Na^+, Na^+−K^+-ATPase, the Na^+−H^+ Exchanger, and the Na−Ca^{2+} Exchanger. *J. Neurosci.* **1996**, *16*, 545−552.

(5) Bensimon, G.; Lacomblez, L.; Meininger, V. The ALS/Riluzole Study Group. A Controlled Trial of Riluzole in Amyotrophic Lateral Sclerosis. *N. Engl. J. Med.* **1994**, *330*, 585−591.

(6) (a) Goldin, S. M.; Subbarao, K.; Sharma, R.; Knapp, A. G.; Fischer, J. B.; Daly, D.; Durant, G. J.; McBurney, R. N.; Reddy, N. L.; Hu, L.-Y.; Magar, S.; Pearlman, M.; Chen, J.; Graham, S. H.; Holt, W. F.; Berlove, D.; Margolin, L. D. Neuroprotective Use-Dependent Blockers of Na^+ and Ca^{2+} Channels Controlling Presynaptic Release of Glutamate. *Ann. N. Y. Acad. Sci.* **1995**, *765*, 210−229. (b) Stys, P. K.; Waxman, S. G.; Ransom, B. R. Ionic Mechanism of Anoxic Injury in Mammalian CNS White Matter: Role of Na^+ Channels and Na^+−Ca^{2+} Exchanger. *J. Neurosci.* **1992**, *12*, 430−439. (c) Stys, P. K. Anoxic and Ischemic Injury of Myelinated Axons in CNS White Matter: From Mechanistic Concepts to Therapeutics. *J. Cereb. Blood Flow Metab.* **1998**, *18*, 2−25.

(7) (a) Yamasaki, Y.; Kogure, K.; Hara, H.; Ban, H.; Akaike, N. The Possible Involvement of Tetrodotoxin-Sensitive Ion Channels in Ischemic Neuronal Damage in the Rat Hippocampus. *Neurosci. Lett.* **1991**, *121*, 251−254. (b) Lysko, P. G.; Webb, C. L.; Yue, T.-L.; Gu, J.-L.; Feuerstein, G. Neuroprotective Effects of Tetrodotoxin as a Na^+ Channel Modulator and Glutamate Release Inhibitor in Cultured Rat Cerebellar Neurons and in Gerbil Global Brain Ischemia. *Stroke* **1994**, *25*, 2476−2482.

(8) Dorman, P. J.; Counsell, C. E.; Sandercock, P. A. G. Recently Developed Neuroprotective Therapies for Acute Stroke. A Qualitative Systematic Review of Clinical Trials. *CNS Drugs* **1996**, *5*, 457−474.

(9) Reddy, N. L.; Connaughton, S.; Daly, D.; Fischer, J. B.; Goldin, S. M.; Hu, L. H.; Subbarao, K.; Durant, G. J. Synthesis and Characterization of *N*-(acenaphthyl-4-yl)-*N*′-(4-methoxynaphth-1-yl)guanidine as a Glutamate Release Inhibitor and Potential Anti-Ischemic Agent. *Bioorg. Med. Chem. Lett.* **1995**, *5*, 19, 2259−2262.

(10) (a) Dong, L. P.; Wang, T. Y.; Zhu, J. Effects of Carbamazepine on Hypoxic and Ischemic Brain Damage in Mice. *Chung Kuo Yao Li Hsueh Pao* **1994**, *15*, 257−259. (b) Murakami, A.; Furui, T. *Neurosurg.* **1994**, *34*, 1047−1051.
(11) Pauwels, P. J.; Leysen, J. E.; Janssen, P. A. J. Ca^{2+} and Na^{+} Channels Involved in Neuronal Cell Death. Protection by Flunarizine. *Life Sci.* **1991**, *48*, 1881−1893.
(12) Ginsberg, M. D. Efficacy of Calcium Channel Blockers in Brain Ischemia: a Critical Assessment. In *Pharmacology of Cerebral Ischemia*; Krieglstein, J., Ed.; Wissenschaftliche Verlagsgesellschaft: Stuttgart, 1988; pp 65−73.
(13) Bowersox, S. S.; Singh, T.; Nadasdi, L.; Zukowska-Grojec, Z.; Valentino, K.; Hoffman, B. B. Cardiovascular Effects of Omega-conopeptides in Conscious Rats: Mechanisms of Action. *J. Cardiovasc. Pharmacol.* **1997**, *20*, 756−764.
(14) (a) Uchitel, O. D.; Protti, D. A.; Sanchez, V.; Cherksey, B. D.; Sugimori, M.; Llinàs, R. P-type Voltage-dependent Calcium Channel Mediates Presynaptic Calcium Influx and Neurotransmitter Release in Mammalian Synapses. *Proc. Natl. Acad. Sci. U.S.A.* **1992**, *89*, 3330−3333. (b) Bowersox, S. S.; Miljanich, G. P.; Sugiura, Y.; Li, C.; Nadasdi, L.; Hoffman, B. B.; Ramachandran, J.; Ko, C.-P. Differential Blockade of Voltage-Sensitive Calcium Channels at the Mouse Neuromuscular Junction By Novel ω-Conopeptides and ω-Agatoxin-IVA. *J. Pharmacol. Exp. Ther.* **1995**, *273*, 248−256.
(15) Nagy, P. I.; Durant, J. G. Monte Carlo Simulation of the Counterion Effect on the Conformational Equilibrium of the *N*,*N*′-Diphenylguanidinium ion. *J. Phys. Chem.* **1996**, *104*, 1452−1463.
(16) Alagona, G.; Ghio, C.; Nagy, P. I.; Durant, G. J. Theoritical Studies on the Relative Stability of Neutral and Protonated *N*,*N*′-Diarylguanidines in Aqueous Solution Using Continuum Solvent Models. *J. Phys. Chem.* **1994**, *98*, 5422−5430.
(17) The authors propose the term "lockamer" to refer to a rigid or semirigid scaffold which mimics the conformation of one or a set of rotamers of the flexible template from which it is derived. The term "foldamer" has been recently introduced.[18]
(18) Appela, D. H.; Christianson, L. A.; Karle, I. L.; Powell, D. R.; Gellman, S. H. β-Peptide Foldamers: Robust Helix Formation in a New Family of β-Amino Acid Oligomers. *J. Am. Chem. Soc.* **1996**, *118*, 13071−13072.
(19) (a) Mohamdi, F.; Richards, N. G. J.; Guiga, W. C.; Liskamp, R.; Lipton, M.; Caufield, C.; Chang, G.; Hendrickson, T.; Still, W. C. MacroModel − An Integrated Software System for Modeling Organic and Bioorganic molecules Using Molecular Mechanics. *J. Comput. Chem.* **1990**, *11*, 440−467. (b) Still, W. C.; Tempczyk, A.; Hawley, R. C.; Hendrickson, T. Semianalytical Treatment of Solvation for Molecular Mechanics and Dynamics. *J. Am. Chem. Soc.* **1990**, *112*, 6127−6129. (c) Weiner, S. J.; Kollman, P. A.; Case, D. A.; Chandra Singh, U.; Ghio, C.; Alagona, G.; Profeta, S., Jr.; Weiner, P. A New Force Field for Molecular Mechanical Simulation of Nucleic Acids and Proteins. *J. Am. Chem. Soc.* **1984**, *106*, 765.
(20) Reddy, N. L.; Amitay, O.; Berlove, D.; Fan, W.; Fischer, J. B.; Magar, S. S.; Wolcott, T.; Yost, E.; Durant, G. J. *N*,*N*′-Diarylguanidines: Synthesis and Antiseizure Activity in the Audiogenic DBA/2 Mouse Model. 211th American Chemical Society National Meeting, New Orleans, LA, 1996; MEDI 57.
(21) Hu, L. Y.; Durant, G.; Guo, J. Q.; Maillard, M.; Wolcott, T.; Berlove, D. Synthesis and Structure−Activity Relationships of Substituted N-aryl-N-aralkylguanidines as Antiseizure Agents. 214th American Chemical Society National Meeting, Las Vegas, NV, 1997; MEDI 32.
(22) Ishikawa, F.; Watanabe, Y.; Saegusa, J. Cyclic Guanidines. IX. Synthesis of 2-Amino-3,4-dihydroquinazolines as Blood Platelet Aggregation Inhibitors. *Chem. Pharm. Bull.* **1980**, *28*, 1357−1364.
(23) Wanzlick, H.; Lachmann, B.; Schikora, E. Zur Bildung und Reaktivität des Bis-[1.3-diphenyl-imidazolidinylidens-(2)]. *Chem. Ber.* **1965**, *98*, 3170−3176.
(24) Hiltmann, R.; Wollweber, H.; Hermann, G. 2-Amino-1-(chlorophenyl)-2-imidazolines as Birds Repellents. *Chem. Abstr.* **1973**, *78*, 136283n.
(25) Walter, G.; Daniel, H.; Bechtel, W. D.; Brandt, K. New Tetracyclic Guanidine Derivatives with H_1-Antihistaminic Properties. *Arzneim.-Forsch/Drug Res.* **1990**, *40*, 440−446.
(26) (a) Bonin, M.; Chiaroni, A.; Riche, C.; Beloeil, J.-C.; Grierson, D. S.; Husson, H.-P. On the Structure of 2,6-Dicyanopiperidines: a Correction. *J. Org. Chem.* **1987**, *52*, 382−385. (b) Takahashi, K.; Mikajiri, T.; Kurita, H.; Ogura, K.; Lida, H. Stereoselective Synthesis of 1-Substituted 2,6-Dicyanopiperidines and Transformation of 2,6-Dialkylproducts of 1-Phenyl-2,6-dicyanopiperidine to δ-Diketones and Cyclohexenones. *J. Org. Chem.* **1985**, *50*, 4372−4375.
(27) Biggs, B. S.; Bishop, W. S. Decamethylenediamine. *Org. Synth. 3*, 229−230.
(28) (a) Oldham, W.; Johns, I. B. Electron Sharing Ability of Organic Radicals. X. Alpha-Substituted Tetrahydroquinolines. *J. Am. Chem. Soc.* **1939**, *61*, 3289−3291. (b) Goldstein, S. W.; Dambek, P. J. 2-Substituted 1,2,3,4-Tetrahydroquinolines from Quinoline. *Synthesis* **1989**, *3*, 221−222.
(29) Honel, M.; Vierhapper, F. W. Selectivity in the Hydrogenation of 6- and 8-Substituted-Quinolines. *J. Chem. Soc., Perkin Trans. I* **1980**, 1933−1939.
(30) Scherz, W. M.; Fialeix, M.; Fischer, J.; Reddy, N.; Server, A.; Sonders, M.; Tester, B.; Weber, E.; Wong, S.; Keana, J. Synthesis and Structure−Activity Relationships of N,N′-Di-*o*-tolylguanidine Analogues, High-Affinity Ligands for the Haloperidol-Sensitive σ Receptor. *J. Med. Chem.* **1990**, *33*, 2421−2429.
(31) Bae, D. H.; Shine, H. J. Photobenzidine rearrangements. 6. Mechanism of the Photodecomposition of 1,4-diaryl-1,4-dialkyl-2-tetrazines. *J. Org. Chem.* **1980**, *45*, 4448−4455.
(32) Durant, G. J.; Magar, S. S. Prepn. of Substd. Guanidine(s) from Cyanamide and Amine − Using a Lewis Acid Catalyst or by a Non-Catalytic Process in which Steric Hindrance is Reduced by Using a Mono-Substid. Cyanamide. U.S. Patent 5298657.
(33) (a) Scheuer, T.; Auld, V. J.; Boyd, S.; Offord, J.; Dunn, R.; Catteral, W. A. Functional Properties of Rat Brain Sodium Channels Expressed in a Somatic Cell Line. *Science* **1990**, *247*, 854−858. (b) West, J. W.; Scheuer, T.; Maechler, L.; Catteral, W. A. Efficient Expression of Type IIA Na^{+} Channel α Subunit in a Somatic Cell Line. *Neuron* **1992**, *5*, 59−70.
(34) Gordon, D.; Merrick, D.; Auld, V.; Dunn, R.; Goldin, A. L.; Davidson, N.; Catteral, W. A. Tissue-specific Expression of the R_I and R_{II} Sodium Channel Subtypes. *Proc. Natl. Acad. Sci. U.S.A.* **1987**, *84*, 8682−8688.
(35) Ahmed, C. M. I.; Ware, D. H.; Lee, S. C.; Patten, C. D.; Ferrer-Montiel, A. V.; Schinder, A. F.; McPherson, J. D.; Wagner-McPherson, C. B.; Wasmuth, J. J.; Evans, G. A.; Montal, M. Primary Structure, Chromosomal Localization, and Functional Expression of a Voltage-gated Sodium Channel from Human Brain. *Proc. Natl. Acad. Sci. U.S.A.* **1992**, *89*, 8220−8224.
(36) Raysdale, D. S.; Scheuer, T.; Catteral, W. A. Frequency and Voltage-dependent Inhibition of Type IIA Na^{+} Channels, Expressed in a Mammalian Cell Line, by Local Anesthetic, Antiarrhythmic, and Anticonvulsant Drugs. *Mol. Pharmacol.* **1993**, *40*, 756−765.
(37) Reith, M. E. A. [^{14}C]Guanidinium Ion Influx into Na^{+} Channels Preparations from Mouse Cerebral Cortex. *Eur. J. Pharmacol.-Mol. Pharmacol. Sect.* **1990**, *188*, 33−41.
(38) Nachshen, D. A.; Blaustein, M. P. Influx of Calcium, Strontium, and Barium in Presynaptic Nerve Endings. *J. Gen. Physiol.* **1982**, *79*, 1065−1087.
(39) Fisher, J. B.; Goldin, S. M.; Hu, L.-Y.; Katraggada, S.; Knapp, A. G.; Margolin, L. Use of Substd. Guanidine(s) for Modulating Neuro-transmitter Release for Treating e.g. Nerve Cell Death, Alzheimer's and Huntington's Disease, Anxiety, Dementia and Arteriosclerosis. PCT/US92/01050.
(40) (a) Seyfried, T. N. Audiogenic Seizures in Mice. *Fed. Proc.* **1979**, *38*, 2399−2404. (b) De Sarro, G. B.; Nistico, G.; Meldrum, B. S. Anticonvulsant Properties of Flunarizine on Reflex and Generalized Models of Epilepsy. *Neuropharmacology* **1986**, *25*, 695−701.
(41) (a) Catteral, W. A. Structure and Modulation of Na^{+} and Ca^{2+} Channels. In *Challenges and Perspectives in Neuroscience*; Ottoson, D., Ed.; Elsevier Science Publishers B.V.: Amsterdam, New York, 1995; pp 51−75. (b) Kisch, G. E. Na^{+} Channels: Structure, Function, and Classification. *Drug Dev. Res.* **1994**, *33*, 263−276. (c) Catteral, W. A. Structure and Function of Voltage-Sensitive Ion Channels. *Science* **1988**, *242*, 50−60.
(42) (a) Meldrum, B. S. The role of Glutamate in Epilepsy and other CNS Disorders. *Neurology* **1994**, *44*, S14−S23. (b) Anticonvulsant Properties of Flunarizine on Reflex and Generalized Models of Epilepsy. *Neuropharmacology* **1986**, *25*, 695−701.
(43) (a) Reddy, N. L.; Hu, L.-Y.; Cotter, R. E.; Fisher, J. B.; Wong, W. J.; McBurney, R. N.; Weber, E.; Holmes, D. L.; Wong, S. T.; Prasad, R.; Keana, J. F. W. Synthesis and Structure−Activity Studies of *N*,*N*′-Diarylguanidine Derivatives. *N*-(1-Naphthyl)-*N*′-(3-ethylphenyl)-*N*′-methylguanidine: A new Selective Non-competitive NMDA Receptor Antagonist. *J. Med. Chem.* **1994**, *37*, 260−267. (b) Hu, L.-Y.; Guo, J. Q.; Magar, S.; Fischer, J. B.; Burke-Howie, K.; Durant, G. J. Synthesis and Pharmacological Evaluation of *N*-(2,5-disubstituted-phenyl)-*N*′-(3-substituted-phenyl)-*N*′-methylguanidines as *N*-Methyl-D-Aspartate Receptor Ion-channel Blockers. *J. Med. Chem.* **1997**, *40*, 4281−4289.
(44) (a) Trickelbank, M.; Singh, L.; Oles, R. J.; Preston, C.; Iversen, S. D. The Behavioral Effects of MK-801: a Comparison with Antagonist Acting Non-Competitively and Competitively at the NMDA Receptor. *Eur. J. Pharm.* **1989**, *167*, 127−135. (b) Rowley, M.; Leeson, P. D.; Stevenson, G. I.; Moseley, A. M.; Stansfield, I.; Sanderson, I.; Robinson, L.; Baker, R.; Kemp, J. A.; Marshall, G. R.; Foster, A. C.; Grimwood, S.; Trickelbank, M. D.; Saywell, K. L. 3-Acyl-4-hydroxyquinolin-2(1H)-ones. Systemically Active Anticonvulsants Acting by Antagonism at the Glycine Site of the *N*-Methyl-D-Aspartate Receptor Complex.

J. Med. Chem. **1993**, *36*, 3386−3396. (c) Berlove, D.; Amitay, O.; Goldin, S.; Margolin, L.; Holt, W. Glutamate Antagonism Suppresses Audiogenic Seizures in the DBA/2 Mouse. *Soc. Neurosci. Abstr.* **1995**, *21*, 770.13.

(45) Hansch, C.; Bjorkroth, J. P.; Leo, A. Hydrophobicity and Central Nervous System Agents: On the Principle of Minimal Hydrophobicity in Drug Design. *J. Pharm. Sci.* **1987**, *76*, 663−686.

(46) Hansch, C.; Leo, A. *Exploring QSAR: Fundamentals and Applications in Chemistry and Biology*; American Chemical Society: Washington, DC, 1995; pp 387−410 and references therein.

(47) Hersey, A.; Hill, A. P.; Hyde, R. M.; Livingstone, D. J. Principles of Method Selection in Partition Studies. *Quant. Struct.-Act. Relat.* **1989**, *8*, 288−296.

(48) Kubinyi, H. Lipophilicity and Drug Activity. *Prog. Drug Res.* **1979**, *23*, 97−198.

(49) Adveef, A. Assessment of Distribution-pH profiles. In *Lipophilicity in Drug Action and Toxicology*; Pliska, V., Testa, B., van de Waterbeemd, H., Eds.; VCH: New York, 1996; pp 109−139.

(50) Yeh, K. C.; Higuchi, T. C. Oil−Water Distribution of p-Alkylpyridines. *J. Pharm. Sci.* **1976**, *65*, 80−86.

(51) (a) Perlman, M. E.; Zhang, L.; Hu, L.-Y.; Reddy, N. L.; Fischer, J. B.; Durant, G. J. Use of pH dependence of log *D* for pK_a determination and formulation of diarylguanidines. *Pharm. Res.* **1996**, *13*, S-33. (b) Perlman, M. E.; et al. Unpublished results.

(52) Pauletti, G. M.; Perlman, M. E.; Zhang, L.; Borchardt, R. T. Can Counterions Affect the Transport of a Lipophilic Diarylguanidine (CNS 1237) Across CACO-2 Cell Monolayers In Vitro ? *Pharm. Res.* **1997**, *14*, S-24.

(53) Irwin, G. M.; Kostenbauder, H. B.; Dittert, L. W.; Staples, R.; Misher, A.; Sintosky, S. V. Enhancement of Gastrointestinal Absorption of a Quaternary Ammonium Compound by Trichloracetate. *J. Pharm. Sci.* **1969**, *58*, 313.

(54) Davis, M. G.; Manners, C. M.; Payling, D. W.; Smith, D. M.; Wilson, C. A. Gastrointestinal Absorption of the Strongly Acidic Drug Proxicromil. *J. Pharm. Sci.* **1984**, *73*, 949−953.

(55) Scherrer, R. A. The Treatment of Ionizable Compounds in Quantitative Structure−activity Studies with Special Consideration to Ion Partitioning. In *Pesticide Synthesis Through Rational Approaches*; ACS Symp. Ser. No. 255; Magee, P. S., Kohn, G. K., Menn, J. J., Eds.; American Chemical Society: Washington, DC, 1984; pp 225−246.

(56) Austin, R. P.; Davis, A. M.; Manners, C. N. Partitioning of Ionizing Molecules between Aqueous Buffers and Phosphoplipid Vesicles. *J. Pharm. Sci.* **1995**, *84*, 1180−1183.

(57) Still, C. W.; Kahan, M.; Mitra, A. Rapid Chromatographic Technique for Preparative Separation with Moderate Resolution. *J. Org. Chem.* **1978**, *43*, 2923−29256.

(58) Nutaitis, C. F. A Convenient One-Pot Synthesis of Symmetric Secondary and Tertiary Vicinal Diamines. *Synth. Commun.* **1992**, *22*, 1081−1085.

(59) Albert, A.; Serjeant, E. P. *The Determination of Ionization Constants*, 3rd ed.; Chapman and Hall: New York, 1984.

JM980124A